Distributed Frequency Regulation System for Interconnected Microgrids Based on Heterogeneous Agent Theory

Billy Wladimir Toro Tovar

Universidad Nacional de Colombia
Facultad de Ingeniería Eléctrica
Bogotá, Colombia
2017

Distributed Frequency Regulation System for Interconnected Microgrids Based on Heterogeneous Agent Theory

Billy Wladimir Toro Tovar

Tesis o trabajo de grado presentada(o) como requisito parcial para optar al título de:
Magister en Ingeniería Elétrica

Director(a):
Ph.D. Eduardo Mojica-Nava

Línea de Investigación:
Control Distribuido
Grupo de Investigación:
PAAS-UN

Universidad Nacional de Colombia
Facultad de Ingeniería Elétrica
Bogotá, Colombia
2017

Dedicado a mis padres, que me apoyaron y tuvieron paciencia durante el desarrollo de todos mis estudios, a Lina que me motivo a dar este importante paso, y a mis compañeros del PAAS-UN en quienes encontré todo el apoyo y amistad para ser mejor.

Acknowledgments

Agradezco al grupo de investigación PAAS-UN y al doctor Eduardo Mojica-Nava, profesor asociado de la Universidad Nacional de Colombia en la facultad de ingeniería. Cuya visión estableció las bases para el comienzo y desarrollo de esta investigación.

Abstract

The increase in the use of distributed energy resources such as photovoltaic panels and wind turbines and the development of most efficient energy storage systems has allowed the implementation of microgrids. This concept includes a geographical area in which storage, generation, and loads can be operated connected or islanded of the distribution network. A microgrid can be AC or DC according to the current in the common bus. In an AC microgrid inverters are required due to the nature of some distributed energy resources; this implies the regulation of voltage and frequency. It can be done either using a centralized method which involves the use of a very reliable communication system or using an entirely decentralized model in which each agent (in this case each inverter) do not communicate with the others. An intermediate approach allows each agent communicate with its neighbors without the needing of a complex communication network. Frequency regulation must guaranty the same value for the whole system, for this purpose consensus equation is used. This method is used to regulate not only the frequency and the voltage for the inverters inside a microgrid but the frequency in several interconnected microgrids. This consensus approach supposes that each agent is identical to the others without having into account the particularities of each one. A frequency regulation method for a microgrids cluster is simulated and verified using a non-identical agent approach.

Keywords: microgrid, cluster, consensus, regulation, frequency, non-identical, agent

Resumen

El aumento en el uso de fuentes distribuidas de energía y recursos de almacenamiento distribuido en las últimas décadas tales como paneles solares, turbinas de viento y bancos de baterias, ha permitido el desarrollo del concepto de Microrred. Una microrred, que agrupa generadores y almacenamiento distribuidos, puede funcionar en AC o DC dependiendo del su bus común. La microrred es definida por un área geográfica capaz de suplir su propia demanda incluso cuando funciona desconectada del sistema de potencia convencional. En un escenario futuro, varias microrredes en modo isla, podrán conectarse entre ellas formando un grupo o 'cluster'. En este trabajo se presenta un sistema de regulación de frecuencia para un grupo de microrredes. Se propone un control jerárquico distribuido basado en teoría de agentes heterogéneos, es decir, agentes no-idénticos. Este control permite la conexión y desconexión de microrredes en el nivel más alto, o la conexión y desconexión de inversores en un nivel inferior. El sistema y sus controladores son verificados por simulación.

Palabras Clave: microrred, cluster, consenso, regulación, frecuencia, no-identicos, agentes

Table of Contents

List of Figures

List of Tables

1. Introduction

Distribution power system has been changing in the last decades; this system is no longer only the link between the transmission network and the users connected to a medium and low voltage (without forgetting its regulation and control functions). Nowadays, distribution system must support distributed energy resources and storage systems, active load release, demand management, and economic dispatch. This network has to evolve to the Smart Grid (SG) [1] using information, measurement, and control devices.

A SG is a huge system that covers an extensive geographic space. It involves not only hardware appliances, but a new concept to organize in levels each technology present in there. To carry out the SG requires the effort of different areas, one of them is to create the MG (Microgrid) [2]. These smaller units that gather DERs (Distributed Energy Resources), DSS (Distributed Storage Systems), control and load release, regulation, etc. interact with the utility network and will be the core unit to build the SG [2].

A fundamental feature of MGs is their capability to work (supply the loads) even when is isolated from the utility [3]. When a MG is connected to the utility works as a load and a current source; DERs can load the DSS or deliver energy to the network, in this case, the utility network determines the stability of the MG. In a MG, isolated from the utility network, stability and regulation problems are critical; the system must guaranty the continuity of the service (at least for the critical loads) with suitable quality margins [3].

A MG can be classified either as AC (Alternating Current) or DC (Direct Current) according to its common bus (The point in which generators and storage systems are connected). Photovoltaic generators and battery banks work in DC, others like wind turbines and flywheel systems work in AC. Both cases require the use of AC-DC or DC-AC converters. Besides, there are the called hybrid MG that employ the two types of conversion [4].

In any isolated microgrid, power sharing is a desirable condition; this feature allows each inverter share power according to its maximum power range. In a DC MG, a variable to achieve power sharing is voltage, which implies the problem of not having a constant resistance value at the DC bus [5]. In an AC MG voltage and frequency must be regulated to establish an appropriate power sharing, depending on the transmission line behavior (resistive or inductive) active and reactive power can be decoupled and controlled making some

variations on frequency or voltage [6].

Hierarchical control sets a standard frame to control a Microgrid. Usually, three levels have been established to fulfill the objectives of the MG [7]. The first level sets the power sharing condition for all inverters inside the microgrid, while the second level is in charge of the MG achieve its voltage and frequency set points at steady state. The third level controls the power flow between the MG and the utility or between the MG and other MG, and sets the conditions for economic dispatch and optimization objectives.

Secondary control can achieve its objectives using either a centralized or distributed approach. Centralized control needs a sophisticated communication system and is susceptible to failures, while distributed secondary control strategy is based on multi-agent theory, which allows that each inverter generates its control signals based on local information. This way, a simpler communication system is required and is less susceptible to failures [8].

Distributed secondary control defines the generators as agents and the communication between them as edges, control signals are generated based on consensus equation [9]. Similarly, tertiary control generates control signals to achieve power sharing among microgrids in a distributed way. In this case, microgrids are defined as agents and communication links as edges. In both cases, inverter and microgrids are considered as identical agents (homogeneous).

To achieve consensus between non-identical agents, it is necessary the use of heterogeneous agents theory [10]. This theory has shown to be a useful tool to reach consensus among agents such as robots and unmanned aerial vehicle (UAVs) [11]. Its field has extended to other areas such as computer science, economy, and biology. In a microgrid, several non-identical behaviors can be found, such as different filter constant times, inverter gains, transmission lines values, even similar devices can have different tolerances and ranges of operation [12].

This work is oriented to the design of a distributed control for inverter and microgrid agents, to regulate frequency and to guaranty power sharing based on heterogeneous multi-agent theory. The control relies on the active power-frequency relation and is capable to guaranty the stability of the system. Factors that make the agents non-identical and their effect in the consensus are considered and compared with a network of identical agents. Even though other studies have been made for inverter based microgrids, the control of an AC microgrid cluster has not been studied profusely and is the principal contribution of this work. Chapter 2 presents the basic concepts of AC microgrids, hierarchical control, and distributed control. The fundamental concepts of graph theory, homogeneity and heterogeneity definitions, inverter and cluster modeling is presented in chapter 3. Simulation for identical on non-identical inverters for several cases plus the simulation of a microgrid cluster and the

effects of some variables in consensus achievement are shown in chapter 4. Finally, conclusions and recommendations are presented in chapter 5. This work is developed based on control theory developing a mathematical model of the whole system first, then is verified by software simulation.

2. Microgrids

A microgrid is a set of distributed energy resources (DERs), loads and protection elements work as a controllable system [2]. DERs include distributed generation (DG) and distributed storage (DS) [3]. This system can operate in two different modes known as connected mode when the microgrid works connected to the utility network and islanded mode (standalone) when the microgrid works isolated from the utility.

A microgrid has a basic structure in which there is a transformer to connect the whole set to the utility network. The point of common coupling (PCC) is a key point before the main transformer that allows to connect or disconnect the microgrid to the utility network, or in some cases to other microgrids. The common bus is the point at which every feeder is connected and where the PCC is located. Each feeder can have its protection and breaker system that allow isolating branches inside the microgrid in case of a fault or a scheduled maintenance [2], [3].

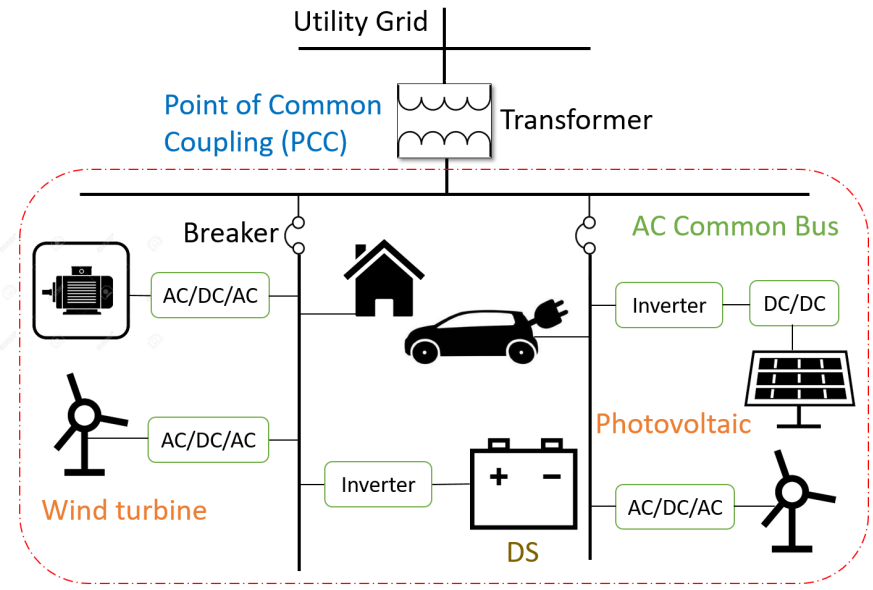

Figure 2-1.: AC microgrid

The common microgrid bus can be either DC or AC defining the type of microgrid. Thus, DERs can be connected to the main bus either directly or by using inverters or rectifiers de-

pending on the case. Among some DERs with AC direct output are included wind turbines, wave and tidal turbines, low-head hydro, and biogas [13]. In contrast, most of the storage devices have DC output, same way that solar panels and fuel cells.

Figure **2-1** shows the way as DERs and loads are connected to an AC microgrid. Some DC sources use DC/DC converters as a first stage and then a DC/AC stage to connect to the common bus. AC DERs utilize in some cases a stage of AC/DC/AC conversion to fix reference values of voltage and frequency.

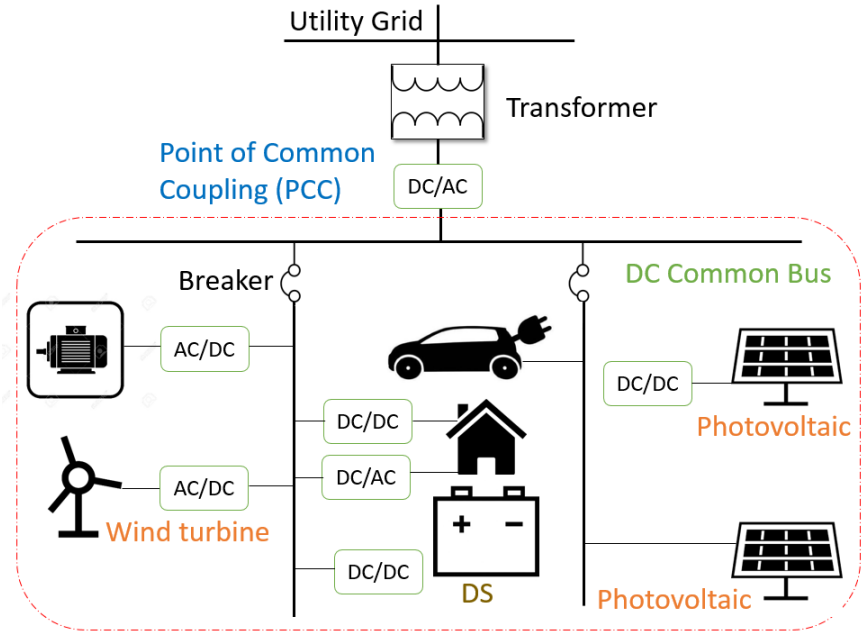

Figure 2-2.: DC microgrid

Figure **2-2** shows a general schematic of a DC microgrid. In this case, DC DERs such as solar panels arrays and DSs need a DC-DC stage to elevate the voltage at the level of the common bus. AC DERs need an AC-DC converter or rectifier stage to achieve the desired voltage level. Other elements such as DC loads can be connected directly to the feeders.

A microgrid connected to the utility network can either supply all the power demanded or been supplied by the main power network. If the microgrid generates an excess of energy, this can be injected into the utility network. In this scenario, the reference values of voltage and frequency are set by the main network. In contrast, an islanded microgrid can choose their reference values according to the power demanded and the availability to generate enough energy.

2.0.1. Smart Grids and Microgrids

The SG is the evolution of the current grid enhancing it rather than replacing it. By definition, the smart grid is a set of concepts, models, and technologies. It allows obtaining an entirely integrated system from generation to consumption, where all the agents of that chain interact exchanging data and services; using communication technologies, involving several generation options such a renewable energy resources and storage systems, and encouraging the users to manage their energy consumption. The future grid will have a self-healing capacity allowing it to avoid or lessen the effects of a failure[14].

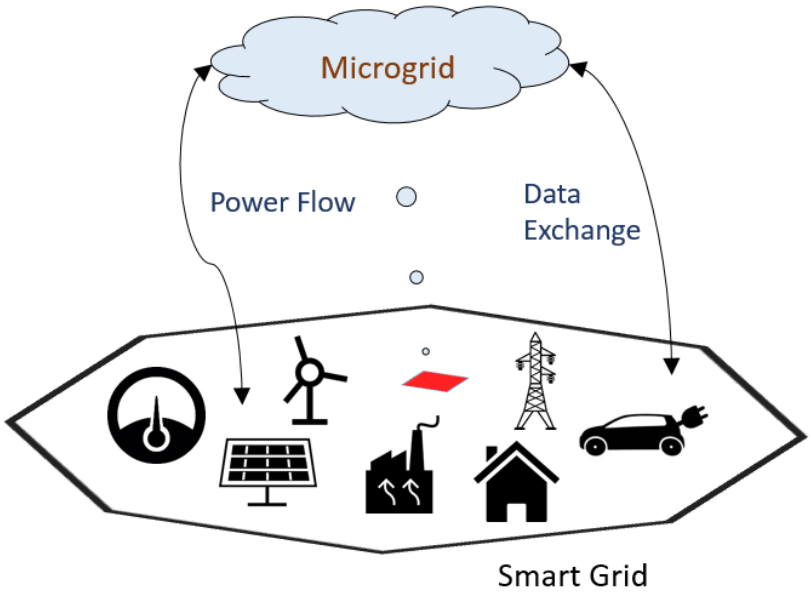

Figure 2-3.: Microgrid as part of the smart grid

The implementation of the microgrids is an essential aspect to build the smart grid [15]. This plug and play structures will allow achieving some of the main goals of the smart grids [14]. Microgrid implementation can bring significant benefits to customers and utilities, such as voltage and frequency regulation, reliability improvement, power quality increasing, and power supply for critical loads. Additionally, the use of DERs located close to the consumers reduces the losses in transmission and distribution lines [13].
As Figure **2-3** and Figure **2-4** show, the microgrid will be part of the future Smart Grid, exchanging power and data with other agents of the system and especially with other microgrids allowing an easier integration.

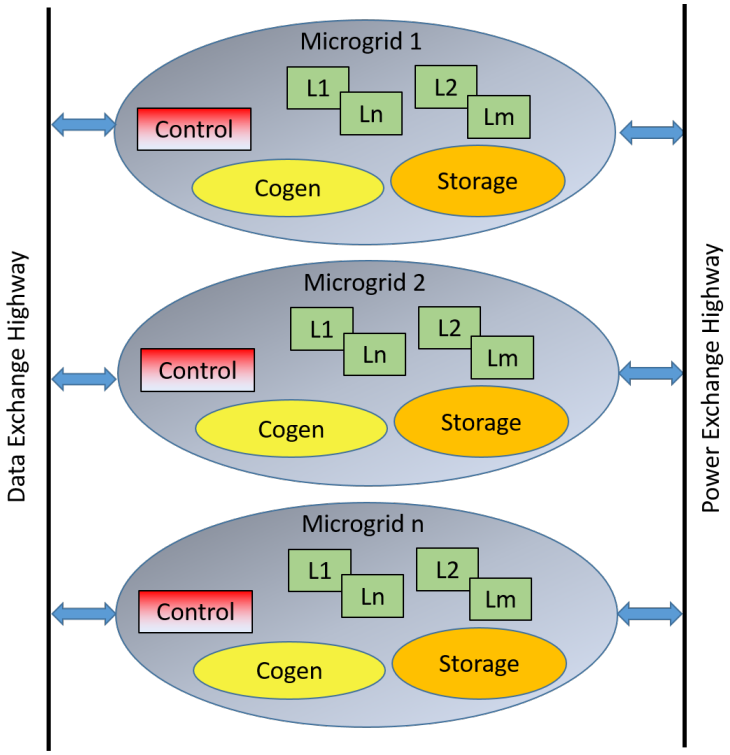

Figure 2-4.: Microgrid cluster power and data exchange [14]

2.1. Control in AC Microgrids

The control of a microgrid involves several challenges since its multi-functional nature. No matter the type of microgrid (AC or DC) it is necessary to follow a standard to achieve a good integration and control inside the microgrid and between the microgrid and the power system. Following this direction, the standard proposed by [7] adapts the ISA-95 to the microgrid's control. Here, a hierarchical control based on three levels is presented. In this common frame, the first level or lower level carries out the regulation and control of physical variables such as voltage, current, and frequency for a single inverter and the way in which several inverters are connected in parallel. The second level guarantees that voltage and frequency are at their reference values. The last level or third level is in charge of energy and power management either between the microgrid and the utility grid or the microgrid and other microgrids.

In the following subsections, three control levels will be explained in better detail.

2.1.1. Primary Control

An AC microgrid is fundamentally based on inverters, in fact, DERs (Distributed Energy Resources) works with this kind of devices. Some microgrids can include synchronous ge-

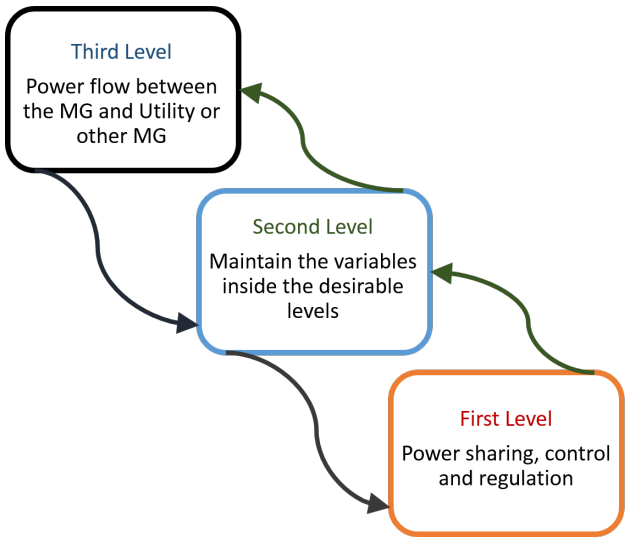

Figure 2-5.: Hierarchical control for microgrids

nerators connected directly to the AC bus. However, many of them include AC/DC/AC converters to get better control and isolation of the fluctuations from the machine. To connect several inverters in parallel bring the same problems as to connect sources in parallel, generating high circulating currents and making the system unstable. Because of this, is introduced a primary control that slightly modified the voltage and frequency (or phase) of the inverter to connect it with the others. An inverter can be controlled according to two strategies: PQ (Active Power-Reactive Power) and VSI (Voltage Source Inverter). In PQ mode the inverter is controlled to supply a determine active and reactive power. In VSI mode the inverter is controlled to supply a load with predefined values of voltage and frequency [6].

An inverter controlled with the VSI strategy emulated the behavior of a synchronous machine. Thus, when several inverters are connected in parallel, each inverter artificially droop its frequency and voltage following a linear relation with active and reactive power [16]. Another important feature desirable in a microgrid is **power sharing**, this property guarantees that each inverter supply power according to its maximum power.

When two AC sources are connected in parallel, some generalizations can be made about their behavior.
Figure **2-6** shows the connection of an inverter to an AC common bus, where ϕ represents the phase angle between the inverter and the bus, E, and V represent the voltage magnitude of the inverter and the bus, respectively. Z is the magnitude, and θ is the angle of the impedance of the transmission line. The following equations represent the active and reactive power that flows from the source to the bus:

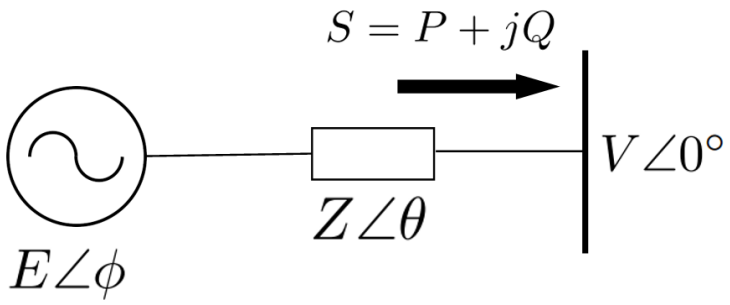

Figure 2-6.: Inverter connection to a common AC bus

$$P = \frac{EV}{Z}\cos(\theta - \phi) - \frac{V^2}{Z}\cos\theta \tag{2-1}$$

$$Q = \frac{EV}{Z}\sin(\theta - \phi) - \frac{V^2}{Z}\sin\theta \tag{2-2}$$

The impedance angle determines the behavior of the microgrid and the way in which it is controlled. Next, the scenarios for predominantly inductive or resistive transmission lines are presented.

Predominantly Inductive Transmission Line

For highly inductive transmission lines (commonly high voltage) with $Z\angle\theta = X\angle 90°$ where X represents the reactance of the transmission line, from (2-1) and (2-2) the next equations are derived

$$P = \frac{EV}{X}\sin\phi \tag{2-3}$$

$$Q = \frac{EV\cos\phi - V^2}{X} \tag{2-4}$$

It is clear that for a predominantly inductive transmission line, active power has a high dependence on the phase angle of the voltage source. Meanwhile, the reactive power has a strong dependence on the magnitude of the voltage source. Based on (2-3) and (2-4), are obtained two droop equations that represent a linear relation between active power and frequency (P-f) and reactive power and voltage (Q-V).

$$\begin{aligned} \omega &= \omega_{ref} - m_p(P_{max} - P_{ref}) \\ E &= E_{ref} - m_q(Q_{max} - Q_{ref}) \end{aligned} \tag{2-5}$$

where ω and E are the angular frequency and voltage magnitude, respectively. ω_{ref} and E_{ref} are the frequency and voltage references. m_p is the active power-frequency droop coefficient, m_q is the reactive power-frequency droop coefficient, and P_{max} and Q_{max} are the maximum active and reactive power outputs of the inverter, respectively.

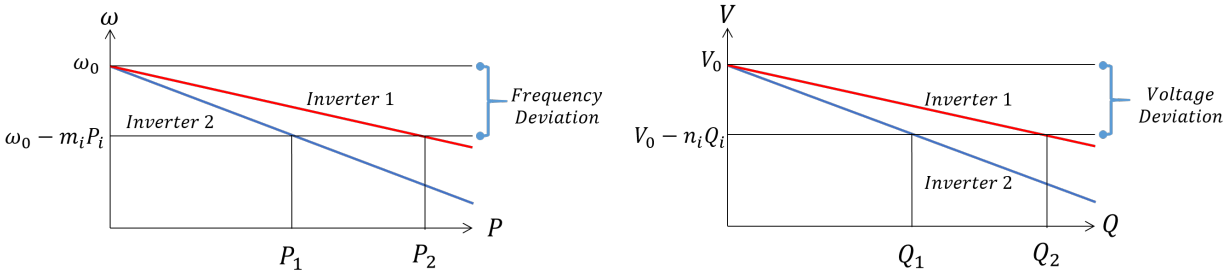

Figure 2-7.: Droop control representation for predominantly inductive lines

When P_{ref} and Q_{ref} are zero, droop equations correspond to the stable state values with ω_{ref} and V_{ref} correspond to not load values [17]. Expression (2-5) becomes

$$\begin{aligned} \omega &= \omega_{ref} - m_p P \\ E &= E_{ref} - m_q Q \end{aligned} \tag{2-6}$$

Figure **2-7** shows the graphs of droop equations for predominantly inductive transmission lines. Droop control introduces frequency and voltage deviations from the reference values, additionally, this method works well with linear loads, but it is not the better option for nonlinear loads [16].

Droop control requires to calculate active and reactive power over one cycle, because of this power is measured and filtered through a low pass filter with a frequency of cut lower than the frequency of the inverter in close loop [16]. Droop control coefficients and filter response determine the dynamics of the control [18], if the m_p value increases, power sharing is achieved, but voltage regulation is affected [16]. Finally, droop control action is limited but the maximum voltage and frequency deviation allowed.

Droop coefficients can be obtained according to (2-7)

$$m_p = \frac{\Delta\omega}{P_{max}}, \qquad m_q = \frac{\Delta E}{Q_{max}} \tag{2-7}$$

At steady state, all the frequencies converge to a common value. The following expression must be satisfied to achieve power sharing and an appropriate frequency control

$$m_1 P_1 = m_2 P_2 = \cdots = m_n P_n \tag{2-8}$$

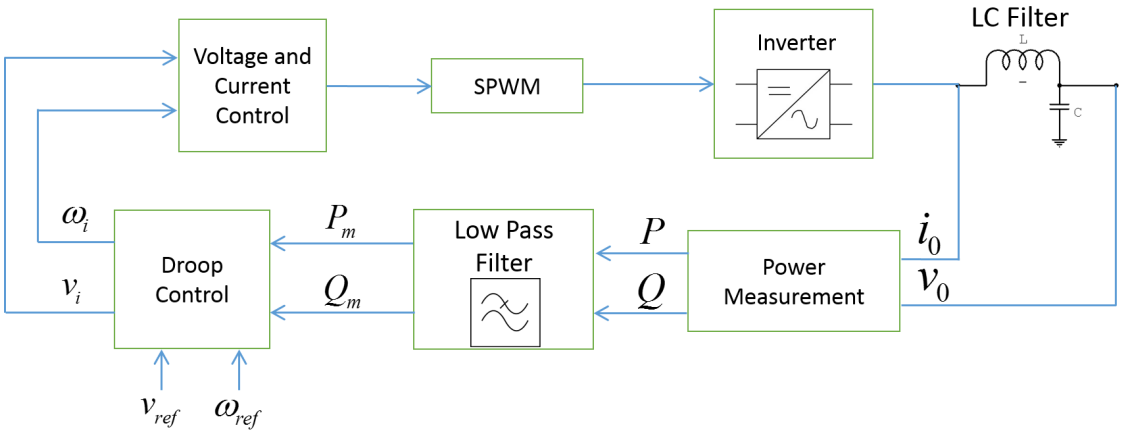

Figure 2-8.: Droop control general scheme

Predominantly Resistive Transmission Line

Impedance in low voltage networks is usually predominantly resistive with $Z\angle\theta = R\angle 0°$, where R represents the resistive part of the transmission line. The next equations are derived

$$P = \frac{EV}{R}\cos\phi - \frac{V^2}{R} \tag{2-9}$$

$$Q = -\frac{EV}{R}\sin(\phi) \tag{2-10}$$

Assuming that the phase difference between the inverter's voltage and the voltage of the bus is almost zero, (2-9), and (2-10) can be simplified as

$$P = \frac{EV - V^2}{R} \tag{2-11}$$

$$Q = -\frac{EV}{R}\phi \tag{2-12}$$

In contrast to the equations for predominantly inductive lines, from (2-11) and (2-12), it is clear that, for predominantly resistive lines, active power has a strong dependence on voltage, while reactive power depends on voltage phase angle. Then, two linear droop equation can be derived

$$\begin{aligned} E &= E_{ref} - m_p P \\ \omega &= \omega_{ref} + m_q Q \end{aligned} \tag{2-13}$$

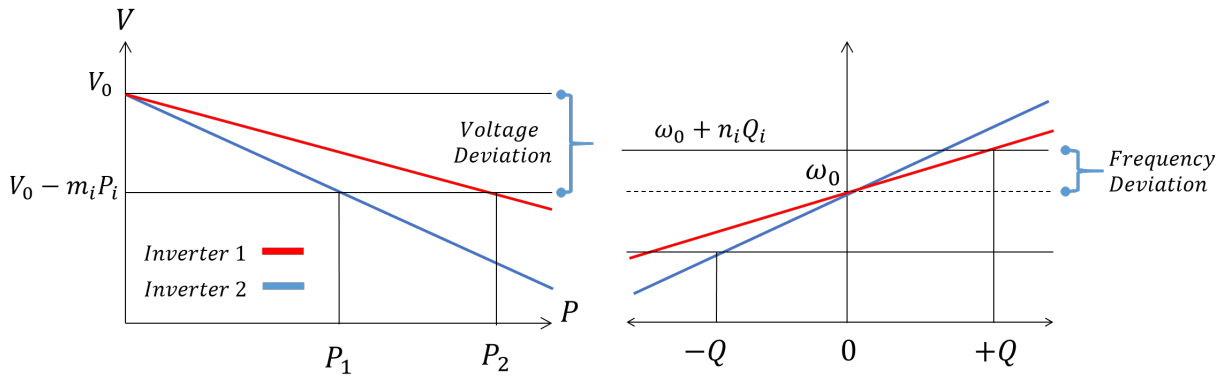

Figure 2-9.: Droop control representation for predominantly resistive lines

Figure **2-9** shows the graph for the predominantly resistive droop equation. Notice that the $P - V$ graph has a negative slope while $\omega - Q$ graph has a positive slope, then an increase in reactive power demand will imply an increase in the frequency of the system [19],[20].

Virtual Output Impedance

Transmission lines determine the behavior of the microgrid and the primary control strategy. In a real scenario, the decoupling between active and reactive power assumption is not always true, in any case, the assumption of a highly inductive or resistive line allows to make that generalization. In a high voltage system, the $P - f/V - Q$ decouple holds and allows to control the active power based on frequency (or phase angle) variations. As frequency is considered a global variable, $P - f$ control has an advantage over the $Q - V$ approach, because of voltage variations caused by the resistive differences through the transmission lines, makes difficult an adequate control of power.

As microgrids are systems that work in low voltage, the condition to use the $P - f$ control strategy does not hold, and the power sharing is inefficient. But, instead of use the $V - Q$ approach, an additional control loop can be used (see Figure **2-10**), this allows to keep the condition of a low reactive-resistive ratio ($\frac{R}{X} \approx 0$) at the output impedance of each inverter.

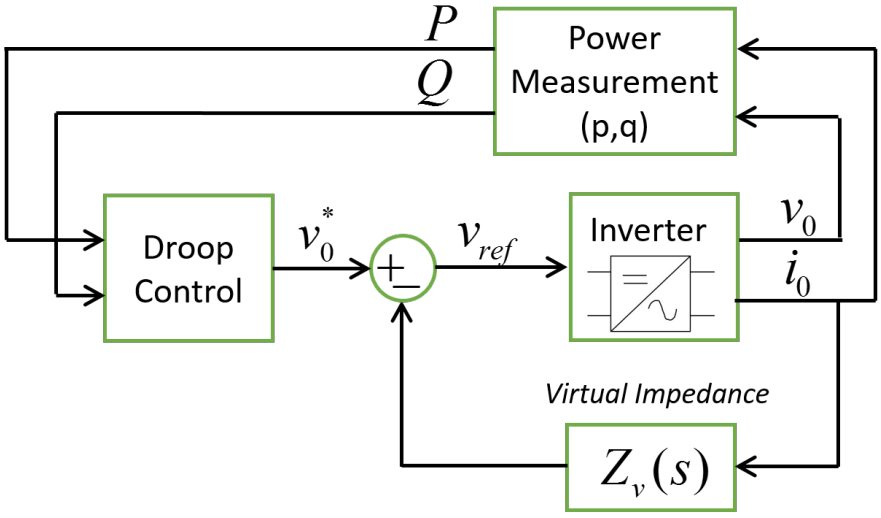

Figure 2-10.: Virtual impedance implementation scheme

Virtual impedance lies in a voltage control feedback term proportional to the output current of the inverter. The output current value is multiplied by the value of the virtual impedance, as is shown in (2-14)

$$v_{ref} = v_0^* - Z_v(s) i_0, \tag{2-14}$$

where v_0^* is the output voltage value of the droop controller, i_0 is the output current value, and $Z_v(s)$ is the virtual impedance. This last value can be chosen according to different criteria depending on the response that is expected and the type of loads that will be connected to the system. As an important design aspect, the virtual impedance must be larger than the impedance of the transmission line to have a significant effect.

The first approach to the virtual impedance design is to set it as $Z_v(s) = sL_v$, following the behavior of inductance to current changes. The voltage in the inductance is given by $V_L = L_v \frac{di}{dt}$, where L_v is the inductance value. This approach can be improved if the virtual impedance is design to respond to the current harmonics when nonlinear loads are connected, equation (2-14) is modified as follows [20]

$$v_{ref} = v_0^* - s \sum L_{Vh} I_h$$

where I_h is the hth current harmonic, and L_{Vh} is the inductance associated with I_h. This way, each current harmonic has associated an inductance value. This method is useful for improving the virtual impedance response. However, THD for nonlinear loads is usually

high; this can be adjusted setting a low-pass filter. The virtual impedance loop is modified as follows [21]

$$v_{ref} = v_0^* - sL_V \frac{1}{s+\omega_c} i_0, \tag{2-15}$$

where ω_c is the cut-off frequency of the low-pass filter, which can be set around 150 Hz and 300 Hz [21].

Angle Droop Control

Voltage angle can be droop instead of the frequency of the system, similarly to classical droop control. Among the advantages of this method are the lack or considerably fewer deviations from the frequency of reference, and the achieving of power sharing in a decentralized way. The voltage angle is modified according to the next equation [22]

$$\delta_0 = \delta_n - m_\delta P, \tag{2-16}$$

where δ_n is the reference angle when the system is supplying a load at its rated power value, m_δ is the angle droop coefficient. Coefficients should be chosen carefully; a high droop coefficient guarantees a good power sharing, in spite of the network parameters, but can make the system unstable [23]. As in droop control, there is a relation among angle droop coefficients and the measured active power

$$m_{\delta_1} P_1 = m_{\delta_2} P_2 = \cdots = m_{\delta_i} P_i$$

Angle droop coefficient can be selected according to the relation between the maximum phase deviation and the rated active power [24] as it is shown next

$$m_\delta = \frac{\Delta\delta}{P_{max}} \tag{2-17}$$

Deviations introduced by angle droop are smaller than in frequency droop. However, angles must be measured based on a common frame, which makes necessary the use of a GPS or other synchronized clock signal [25]. Another strategy to synchronize the generated signals is to achieve a common value in which all signal converge; this can be made using the consensus equation as it is shown in the next section.

2.1.2. Secondary Control

Droop control is a useful method to connect several inverters in parallel and to achieve power sharing, but it introduces some voltage and frequency deviations from their reference values.

According to the hierarchical control strategy, a secondary control loop can fix the deviations introduced by primary control. Secondary control law can be seen as an additional term that moves the linear response of droop control equations vertically as follows

$$\omega_i = \omega_{ref} - mp_i + \delta\omega_i$$
$$E_i = E_{ref} - mq_i + \delta E_i$$

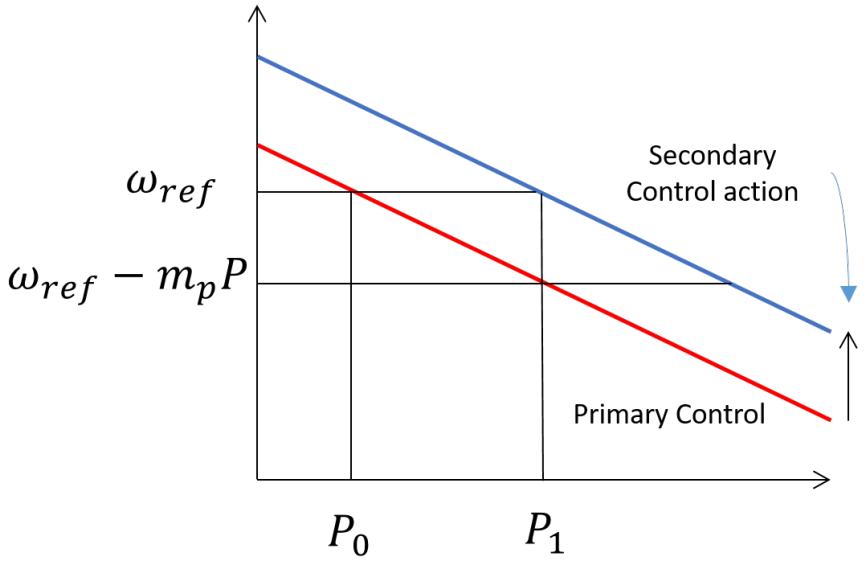

Figure 2-11.: Secondary control action over droop control

Figure **2-11** shows the action of secondary control. The slope of the equation is the same, and its response must be slower than the response of primary control. Which is important to ensure decoupling between the controllers.

Secondary control can be centralized, decentralized, or distributed. A controller is said *centralized* if all the decisions are made from a control that gathers the signals of all the agents or devices. A controller is *decentralized* if the decisions are made for each agent without knowing the state of the other agents, and there is no communication between individual controllers. A controller is *distributed* if the decisions are made with limited information, at this case each agent knows only the state of other agents name neighbors [26]. Figure **2-12** shows a diagram that classifies secondary control action according to the way this is implemented in a multi-agent system. Table **2-1** compares secondary control strategies. Thus it is clear that the selected approach must be based on the particular characteristic of each system.

Table 2-1.: Secondary control strategies

Secondary Control			
	Centralized	**Decentralized**	**Distributed**
Signals and Measurements	Gather from the whole system	Only its own	Local (Neighborhood)
Communication System	Complex, susceptible to failure	Not necessary	Less complex, more reliable
Control Capabilities	High. Optimization and other algorithms implementation	Low. Only local improvements	More complex. Difficult to have a global vision
Plug and Play Capacity	Low. New elements requires to make a lot of changes	High. A new element does not require to make changes	Little changes has to be done to introduce new elements

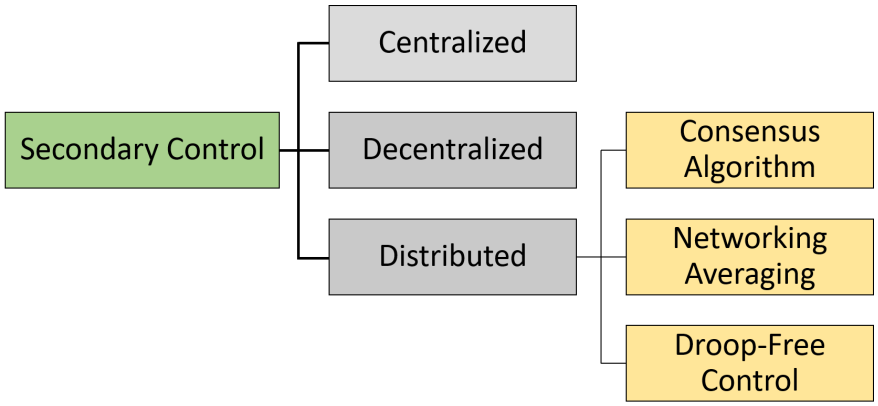

Figure 2-12.: Secondary control classification

Centralized Secondary Control

In a centralized control, the voltage and the frequency of the common bus are measured and then compared with the reference values. The error signal is then processed through a PI controller and send it to all the inverters of the microgrid [7]. As measures and control signals are gathered from all the inverters of the microgrid, communication system should be highly reliable. The secondary control terms can be calculated as

$$\delta\omega_i = k_{p\omega}(\omega^*_{MG} - \omega_{MG}) + k_{i\omega}\int(\omega^*_{MG} - \omega_{MG})dt$$

$$\delta E_i = k_{pE}(E^*_{MG} - E_{MG}) + k_{i\omega}\int(E^*_{MG} - E_{MG})dt$$

where $k_{p\omega}$, $k_{i\omega}$, k_{pE}, and $k_{i\omega}$ are the control gains for frequency and voltage secondary controllers.

Distributed Secondary Control

As a secondary centralized control requires a complicated communication structure, a distributed secondary control is a good option to accomplish the voltage and frequency regulations keeping the power sharing capacity. For frequency regulation, there are different protocols, based on distributed methodology: networking averaging method, and consensus algorithm [27].

Consensus Algorithm In [8] a secondary frequency control is proposed based on consensus algorithm. Here, primary control terms mp_i are used to guaranty the power sharing among units while the ω_i terms are synchronized to the frequency of reference. This method is useful for achieving synchronization and power sharing but has the disadvantage that requires a frequency measurement at each inverter. In general terms, the frequency for the i-th inverter is given by the following expression

$$u_i = -c(\sum_{j\in N_i} a_{ij}(\omega_i - \omega_j) + g_i(\omega_i - \omega_{ref}) + \sum_{j\in N_i} a_{ij}(m_{pi}P_i - m_{pj}P_j))$$

where c is a gain parameter, ω_i and ω_j are the measured frequencies for i and j inverters, respectively. ω_{ref} is the frequency of reference and $m_{pi}P_i$ are the droop value of primary control.

Networking Averaging In [28] is proposed an averaging method for frequency and voltage secondary control. In this case, the secondary control at each inverter takes the measures shared from all the other units: voltage, frequency, and reactive power. Then, the average of that values is calculated and the control signals generated as follows

$$\bar{f}_{DG_K} = \frac{\sum_{i=1}^{N} f_{DG_i}}{N}$$

$$\delta f_{DG_K} = K_{pf}(f^*_{MG} - \bar{f}_{DG_K}) + K_{if}\int (f^*_{MG} - \bar{f}_{DG_K})dt,$$

where i is the number of frequency measurement, and k is the number of inverter units. As it is shown in the last equation, the term $\bar{f}_{DG_K}$ adds an adjusting value to the primary control reference.

This method needs to measure the frequency at sample times. Additionally, each unit needs a good communication system to gather all the frequency measures for the inverters and be capable of calculating a good average frequency value. One of the advantages is its distributed and plug and play capacity, and the power sharing capacity.

Droop-Free Control Another approach to AC microgrid control is proposed by [29], here primary and secondary control act in one single control based on phase deviations rather than frequency droop. This control strategy guaranty the power sharing capacity and, at the same time, the frequency regulation in a distributed way with plug and play capacity.

The droop-free control works for voltage and reactive-power regulation too. The frequency control strategy acts over the phase parameter, the voltage at inverter i is given by the following expression

$$v_i(t) = A\sin(\omega t + \phi) \tag{2-18}$$

where A is the voltage amplitude, ω is the angular frequency, and ϕ is the phase angle.
As frequency control must guaranty an appropriate power sharing, this control method calculates the ratio between the active power measured at each inverter and its maximum power rating. In fact, this is a normalized value as a per unit value without having a global reference. The normalized active power for inverter i is given by

$$P_{norm,i} = \frac{P_i}{P_{max,i}}$$

where P_i is the measured active power for inverter i, and $P_{max,i}$ is the maximum active power available for inverter i. These normalized values are used to get the agreement term using consensus equations as follows

$$\delta_i(t) = c\int_0^t \sum_{j\in N_i} a_{ij}(p_j^{norm} - p_i^{norm})d\tau$$

where N_i is the set of neighbors for agent i, c is a constant gain control value, and a_{ij} correspond to the adjacency value that represents if there is a link between agent i and agent j.

The complete voltage control signal for PWM can be written as

$$v_i(t) = e_i\sin\left(\omega_{rated}t + \int_0^t \delta_i d\tau\right)$$

One of the main advantages of this method is the needless frequency measurement. Its distributed nature guaranty the plug and play condition, and the appropriate power sharing.

2.1.3. Tertiary Control

Tertiary control is the highest level of hierarchical control; it is in charge of the power flow control between the microgrid and the utility network or among islanded microgrids. Besides, tertiary control can manage other functions such as economic dispatch and synchronization. Power flow can be managed by adjusting the voltage and the frequency according to the active and reactive power [20], as it is shown as follows

$$\omega_{ref} = K_{PP}(P_G^{ref} - P_G) + K_{IP}\int (P_G^{ref} - P_G)dt, \tag{2-19}$$

where K_{PP} and K_{IP} are the proportional and integral gains, P_G^{ref} is the active power reference, P_G is the active power measured in the microgrid, and ω_{ref} is the frequency for primary control.

When K_{IP} from (2-19) is equal to zero, the control equation acts as a primary control for the microgrid [30], allowing that several microgrids can be interconnected. Based on this, a droop-free tertiary control is proposed here, this control shifts the phase of the voltage signals according to the power measured and the maximum power rating of each microgrid, maintaining the reference values of voltage and frequency.

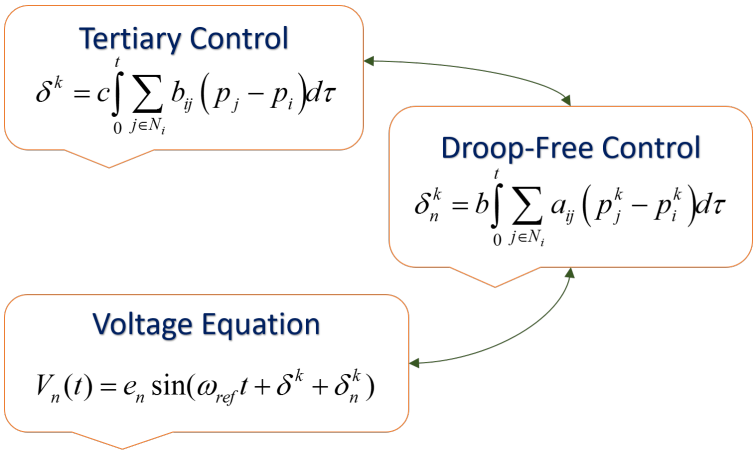

Figure 2-13.: Control signal generation with a tertiary control

Figure **2-13** shows the flow signal among the tertiary control, droop-free control, and signal generator for PWM. Notice that tertiary and secondary control terms are added to the phase term in the voltage equation.

2.1.4. Phase Synchronization

Secondary control is not only in charge of frequency restoration but phase synchronization too. An additional term is included in the equation for secondary control as follows

$$\omega_i = \omega_{ref} - mp_i + \delta\omega_i + \Delta fs_i$$

where Δfs_i is the synchronization term whose value is zero when the voltage values have been synchronized.

A microgrid can be synchronized either to the utility network or other microgrids. In the first case, the voltage magnitude and frequency references are given by the main network. In the second case, the references are generated by each system. Before the connection to the utility or the other microgrid, the voltage phase is sensed and compared with the local phase, varying it slowly until the difference between them is close to zero.

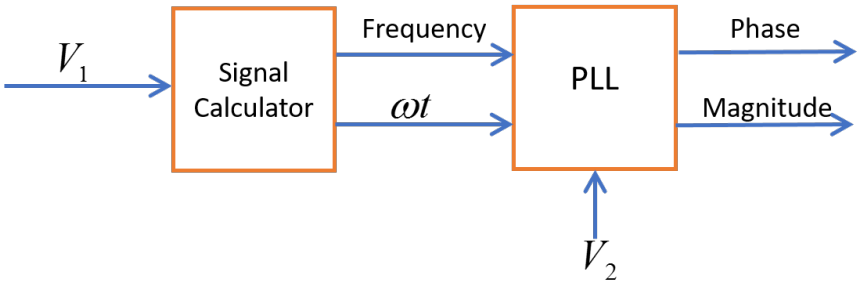

Figure 2-14.: Phase calculation

Figure **2-14** shows how the phase and magnitude is calculated for voltage signal V_1, notice that the phase is measured taking as reference V_2 with a synchronize signal ωt.

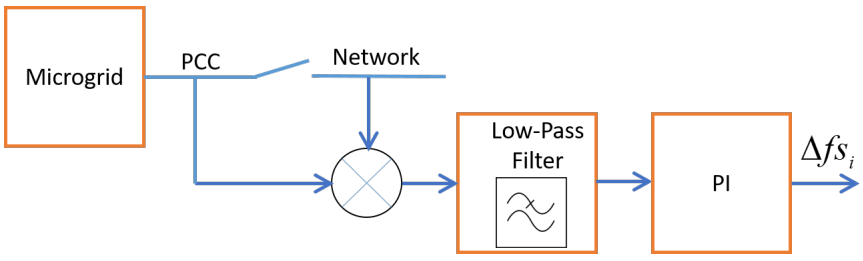

Figure 2-15.: Control of phase before interconnection

Figure **2-15** shows how the phase difference is reduced using a PI controller, the system uses a low-pass filter to eliminate fast phase responses.

2.2. Distributed Storage System

One of the most commonly used storage systems is the battery bank. Batteries are based on several elements, among the most common are the Lithium-Ion and Lead-Acid batteries.

The battery is modeled based on the Shepherd model [31] as a controlled voltage source in series with a constant resistance, the discharge voltage equation is given by the following expression [32]

$$V_{batt} = E_0 - K\frac{Q}{Q - it}it - Ri + Ae^{-Bit} - K\frac{Q}{Q - it}i^*$$

where $K\frac{Q}{Q - it}it$ is denominated the Polarization Voltage, and $K\frac{Q}{Q - it}i^*$ is the Polarization resistance.

Table 2-2.: Battery model parameters

Parameter	
V_{batt}=battery Voltage (V)	A=exponential zone amplitude (V)
E_0 =Battery Constant Voltage (V)	B=exponential zone time constant inverse $(Ah)^{-1}$
K=Polarization constant (V/Ah) or Polarization Resistance (Ω)	R=internal resistance (Ω)
Q=Battery Capacity (Ah)	i=battery current (A)
$it = \int idt$ =actual battery charge (Ah)	i^*=filtered current (A)

The charge dynamic is different depending on the type of battery, for the case of Lead-acid and Lithium batteries have the same behavior. For a Lithium battery, the charge equation is given by the follow expression

$$V_{batt} = E_0 - K\frac{Q}{it - 0{,}1Q}i^* - Ri - K\frac{Q}{Q - it}it + Ae^{-Bit}$$

This model assumes that the value of the internal resistance is constant during the charge and discharge processes. The capacity of the battery is constant in every case, the temperature does not affect the model, there is no memory effect, and the parameters of the battery are deduced from the discharge curves and assumed the same for the charge process [33].
Figure **2-16** shows the typical connection of a battery bank. First, several batteries are connected in series; the output voltage is elevated using a DC-DC dual converter which allows a power flow in both directions. Finally, the high DC voltage is converted to an AC voltage signal at the required frequency and voltage magnitude through a dual inverter.

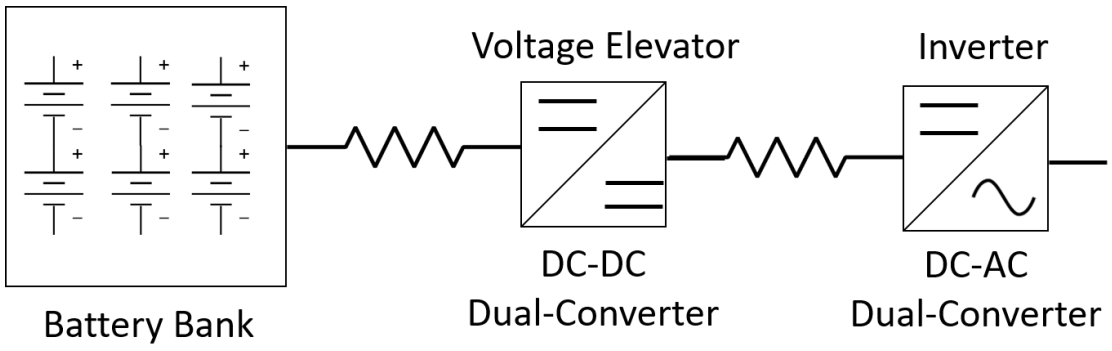

Figure 2-16.: Scheme of connection of a battery bank to a microgrid bus

3. Homogeneous and Heterogeneous Networks

This chapter presents in its first part the fundamental concepts of graph theory, such as spectral properties, and graph Laplacian Potential. Then, the definition of homogeneous and heterogeneous agents are presented. Heterogeneous systems are defined either as agents with time delays or agents with different behaviors; this last problem is solved with a distributed PI control strategy. Based on previous concepts, the frequency control of power system is presented, then some factors that make the agents heterogeneous are considered. Finally, inverter and cluster are modeled and control designed.

3.1. Fundamental Concepts of Graph Theory

Networked system science has attracted the attention of many researchers. A variety of applications has emerged in several disciplines such as biology, aeronautic engineering, economics, and control. In networked systems, each agent has to act according to some standard rules to achieve global objectives. Thus, information and communication are the most important aspects of this kind of systems. Graph theory sets up the basis to analyze networked systems. Graphically, a graph represents the elements in a networked system and the communication links among them. Particularly, those elements are called vertices and links are called edges. Edges of a graph can have a major or minor participation to achieve the global objectives. It can be represented adding a 'weight' function that assigns a constant value to each vertex. This new graph is known as a *weighted graph*.

For the general case, a weighted graph is defined by

$$G = (V, E, w),$$

where V is the vertex set of n elements written as $V = \{v_1, v_2, ..., n\}$, E is the edge set $E = \{e_{ij} = (v_i, v_j)\} \subset V \times V$, and w is a function that assigns a real value to each edge $w : E \to \mathbb{R}$ [34].

According to the communication flow between two nodes, a graph can be classified as *directed* and *undirected*. In an *undirected* graph the communication flow happens in both directions,

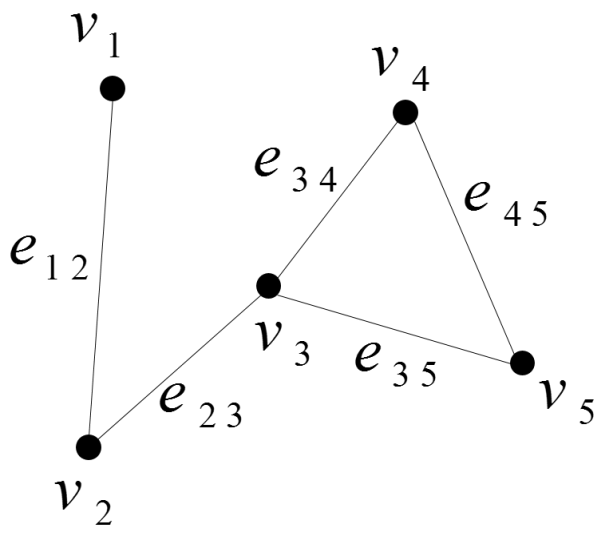

Figure 3-1.: Graph representation

on the contrary the graph is *directed*. Figure **3-1** shows an undirected graph, consisting of five vertexes and five edges.

Two vertices are *adjacent* if they have a common edge. The set of adjacent vertices of vertex i is known as the set of *neighbors* and is represented by $N_i = \{v_j : e_{ij} = (v_j, v_i)\} \in E$, and correspond to those vertices that share information with vertex i, this condition is not fulfilled in a directed graph and depends of the information flow direction.

Adjacency Matrix

This matrix is defined as a symmetric non-negative matrix in which the number of adjacency vertexes are calculated for each vertex of the graph. Mathematically the adjacency matrix is written as $A = [a_{ij}] \in \mathbb{R}^{N \times N}$. $(v_j, v_i) \in E \Leftrightarrow a_{ij} > 0$. Here, if two vertex belong to the edge set, the value of a_{ij} is more than zero. The adjacency term for a vertex itself is equal to zero $a_{ii} = 0$ [34].

Degree Matrix

The *degree* of a vertex, in an undirected graph is the cardinality of the neighborhood set of a vertex i, written as $d(v_i)$. In other words, is the number of adjacent vertices of vertex i. Based on this definition, the *degree matrix*, denoted by $\Delta(G)$ can be defined as the diagonal matrix that contains the degree of its vertices on the diagonal [34].

$$\Delta(G) = \begin{pmatrix} d(v_1) & 0 & \cdots & 0 \\ 0 & d(v_2) & \cdots & 0 \\ \vdots & \vdots & \ddots & 0 \\ 0 & 0 & \cdots & d(v_n) \end{pmatrix}$$

Laplacian Matrix

The Laplacian matrix, in an undirected graph, is defined as the difference between the degree and the adjacency matrices

$$\mathbf{L} = \mathbf{\Delta} - \mathbf{A}$$

Otherwise, the elements of the Laplacian matrix can be defined as

$$L_{ij} = \begin{cases} deg(v_i) & \text{if} \quad i = j \\ -1 & \text{if} \quad i \neq j \\ 0 & \text{otherwise} \end{cases}$$

The rows of the Laplacian matrix sum to zero, being a symmetric and positive semidefinite matrix. It can be written as

$$\mathbf{L1} = \mathbf{0},$$

where $\mathbf{1}$ is a vector of ones $\mathbf{1} = [1, \cdots, 1]$

Graph Definitions and Spectral Properties

A *path* is defined as a sequence of different vertices in a graph that is connected. Thus, a graph is said *connected* if there is a path for every pair of vertices.

An undirected graph in which any pair of vertices are connected by one and only one path is called a *tree*. A *spanning tree* is a subgraph of G, that is also a tree containing all the vertices of the graph.

As Laplacian matrix is symmetric and positive semi-definite, its eigenvalues can be ordered from minor to major, where the first eigenvalue is equal to zero $\lambda_1(G) = 0$. For a connected graph the second smallest eigenvalue is major than zero and is known as the *algebraic connectivity* of a graph [35]. According to the spectral graph theory [34], if a graph has a spanning tree the Laplacian eigenvalue $\lambda_1 = 0$. And the graph G is connected if and only if the second eigenvalue of the Laplacian matrix is $\lambda_2 > 0$.

Consentability: is the capacity of a distributed multi-agent system with consensus protocol to achieve consensus asymptotically.

Scalability: implies that the controller of the system uses only local information at each agent and the scale of the system is usually not important. This way, enhancing the system does not require changes on it [36].

Theorem [36]:
Let G be a weighted digraph of order n. The following statements hold:
1. $\mathbf{L}(G)\mathbf{1}_n = \mathbf{0}_n$, that is, 0 is an eigenvalue of $L(G)$ with eigenvector $\mathbf{1}_n$;
2. For any eigenvalue λ_i, $i = 1, \cdots, n$, of $\mathbf{L}(G)$, either $\lambda_i = 0$ or $Re\lambda_i > 0$. Thus, if G is undirected, then $\mathbf{L}(G)$ is positively semi-definite;
3. Digraph G contains a globally reachable vertex (or an undirected graph is connected) if and only if rank$(\mathbf{L}(G) = n - 1)$.

Graph Laplacian Potential

The concept of potential energy stored in linked systems such as spring-mass and hoist can be emulated in multi-agent systems. At this case, a kind of virtual energy is stored in the graph and depends on its topology. In an undirected weighted graph G with N agents, Laplacian matrix L, and x_i denote the state of agent i, the Laplacian potential is defined as [37]

$$P_L = \sum_{j \in N_i}^{N} a_{ij}(x_i - x_j)^2. \tag{3-1}$$

The potential function (3-1) satisfies the follow identity

$$P_L = \sum_{j \in N_i}^{N} a_{ij}(x_i - x_j)^2 = 2X^\top LX. \tag{3-2}$$

This property can be used as a measure of disagreement among the agents. In fact, lemma 7.4 from [37] establishes that "for a connected undirected graph, $P_L = 0$ if and only if consensus of the multi-agent system is achieved ".

In the case of a single integrator system of N agents $\dot{x}_i = u_i, \quad i = 1, \cdots, N$, where $x_i \in \mathbb{R}$, $u_i \in \mathbb{R}$ are the state and input for agent i, respectively. With consensus equation $u_i = -\sum_{j=1}^{N} a_{ij}(x_i - x_j)$. The whole system is written in matrix form as $\dot{X} = -LX$. Lemma 7.10 from [37] set that if the graph is undirected consensus is reached. This is demonstrated using the Lyapunov candidate function

$$V = \sum_{i=1}^{N} x_i^2 = X^\top X$$

Then $\dot{V} = 2X^\top \dot{X} = -2X^\top LX$. The LaSalle's invariance principle sets that if for a system $\dot{x} = f(x)$ can be found a function $V(x)$ such that $\dot{V} \leq 0$ for all x is negative semidefinite, $V(x) > 0$, for all $x \neq 0$ is positive definite, and $V(0) = 0$, then all the trajectories converge to the largest invariant set in which $\dot{V} = 0$ [38]. Notice that according to the principle V does not need to be necessarily positive definite.

3.2. Homogeneity and Heterogeneity Definition

Consensus problem has been widely studied in recent years. Most of the contributions made in this field have been developed based on the assumption that all the agents have an identical dynamic. Thus, stability analysis is determined by the eigenvalues of the Laplacian matrix [35]. However, in many problems of the real world, each agent shows a different dynamics from the other, and the assumption of homogeneity fail to fulfill.
In networked systems, based on non-identical agents, synchronization problem can be treated in two different ways: *state synchronization*, and *output synchronization*. As agents in a heterogeneous system can have different dimensions to achieve state synchronization, it might be not possible. Thus, output synchronization is a more natural concept [39].

Defining a distributed system of N agents as

$$\begin{aligned} \dot{x}_i(t) &= \mathbf{A}_i x_i(t) + \mathbf{B}_i u(t - T_i) \\ y_i(t) &= \mathbf{C}_i x_i(t) + \mathbf{D}_i u(t - T_i) \qquad i\text{=1,2, ... , } N, \end{aligned} \tag{3-3}$$

where $x_i \in \mathbb{R}^{n_i}$ represents the state, $u_i \in \mathbb{R}$ represents the input variable, and $y_i \in \mathbb{R}$ represents the output value. T_i is the input delay, usually caused by the processing time and the communications packets at each agent.

Each agent inside a network has a local controller represented by the following set of equations

$$\begin{aligned} \dot{\hat{x}}_i(t) &= \mathbf{A}_i^k \hat{x}_i(t) + \mathbf{B}_i^k (r_i(t) - z_i(t)) \\ u_i(t) &= \mathbf{C}_i^k \hat{x}_i(t) + \mathbf{D}_i^k (r_i(t) - z_i(t)) \end{aligned}$$

where $\hat{x}_i \in \mathbb{R}^{m_i}$ is the state of the local controller for i-th agent. $r_i(t)$ is a reference signal for the i-th agent, and $\mathbf{A}_i^k \in \mathbb{R}, \mathbf{B}_i^k \in \mathbb{R}, \mathbf{C}_i^k \in \mathbb{R}$, and $\mathbf{D}_i^k \in \mathbb{R}$ are the parameters of the local controller [36].

Taking the Laplace transform of (3-3), the transfer function for the i-th agent is given by

$$G_i(S) = [\mathbf{C}_i(S\mathbf{I} - \mathbf{A}_I)^{-1}\mathbf{B}_i + \mathbf{D}_i]e^{-T_i S}$$

Same way, taking the Laplace transform for the local controller equation for the i-th agent, the local transfer function is

$$k_i(S) = \mathbf{C}_i^k(S\mathbf{I} - \mathbf{A}_i^k)^{-1}\mathbf{B}_i^k + \mathbf{D}_i^k.$$

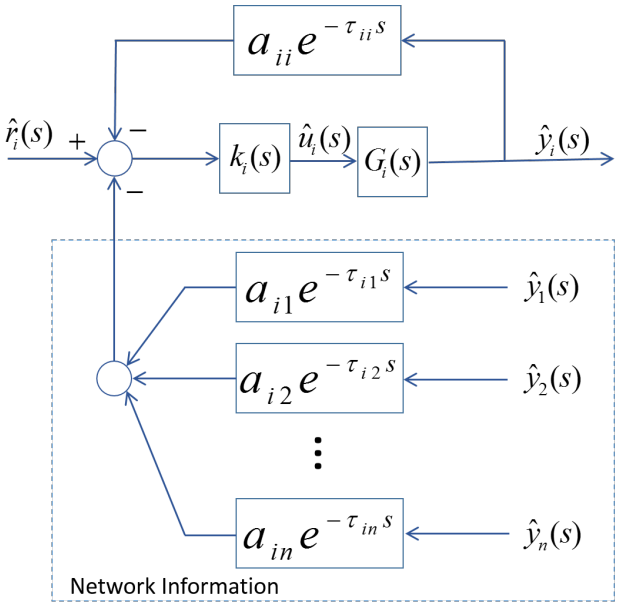

Figure 3-2.: General distributed control schematic for the i-th agent [36]

Figure **3-2** shows the control dynamics for the i-th agent. Notice the local delay $a_{ii}e^{-\tau_{ii}S}$, the other agents delays $a_{ij}e^{-\tau_{ij}S}$, the local controller transfer function $k_i(S)$, and the global transfer function $G_i(S)$.

Figure **3-3** shows the control diagram for whole system. Where $G(S) = diag\{G_i(S)\}$ $i \in \{1, \cdots, n\}$, $K(S) = diag\{k_i(S)\}$ $\quad i \in \{1, \cdots, n\}$, $\Lambda(S) = diag\{a_{ii}e^{-\tau_{ii}S}\}$ $\quad i \in \{1, \cdots, n\}$, and $A(S) + \Lambda(S) = \bar{A}(S)$ with $\bar{A}(S) = a_{ij}e^{-\tau_{ij}S}$. The set of matrices $A(S) + \Lambda(S)$ is a generalized complex adjacency matrix grouping the topology and channel dynamics of the network [36].

Definition: A distributed control system is *homogeneous* if all its agents and the network (graph) are all homogeneous (identical), otherwise if either the agents or the network are not

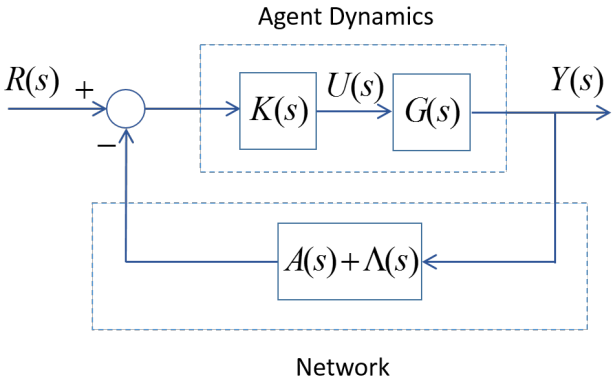

Figure 3-3.: Matrix and block representation of the whole system [36]

homogeneous, the system is *heterogeneous*. The dynamics of the agents are homogeneous if $k_i(s)G_i(s) = k_j(s)G_j(s)$ for $i, j \in \{1, \cdots, n\}$. The $a_{ij}(s) = a_0(s) \in \mathbb{R}H_\infty$ [36].

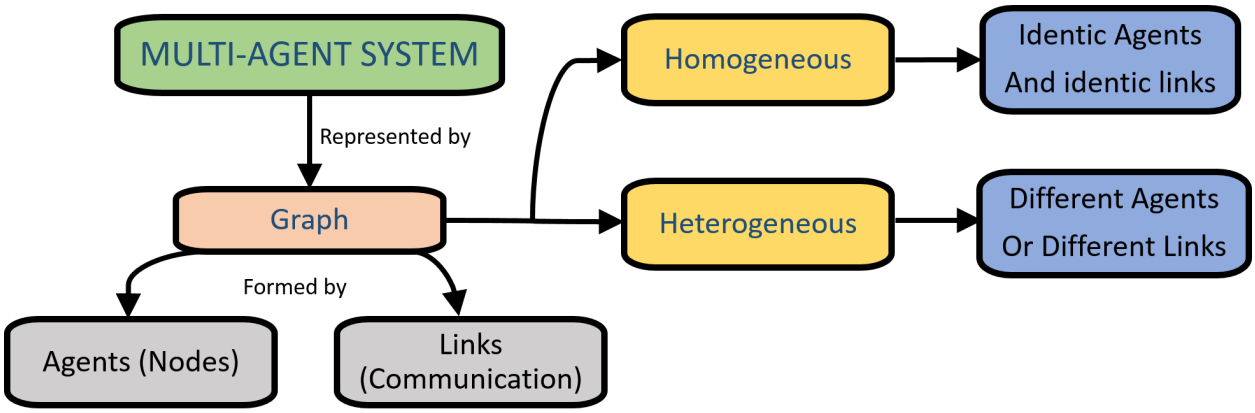

Figure 3-4.: Multi-Agent system classification

Agents in a networked system can be *introspective* and *non-introspective* (see Figure **3-5**). An *introspective* agent has knowledge of its own state and output not matter the other agents. A *non-introspective* agent does not have knowledge of its own states or outputs and requires the interactions with other agent in order to know that data [40].

3.2.1. Internal Model Principle

A necessary condition to synchronize heterogeneous networks is presented in [41]. The condition establishes the existence of a virtual exosystem that generates all the trajectories at which agents converge asymptotically. This way, it is possible to generate a virtual observa-

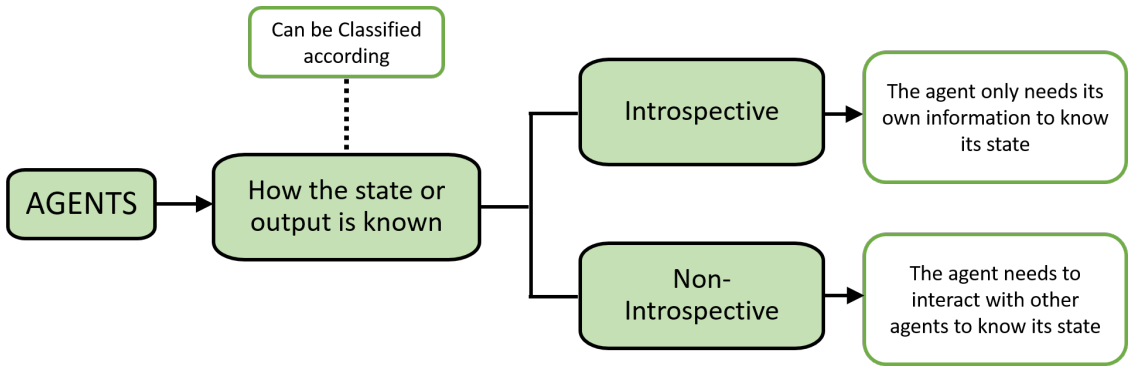

Figure 3-5.: Introspective and non-introspective agents

ble exosystem for each agent and then synchronized the network.

Considering a system of N agents with multiple inputs and outputs defined as

$$\begin{aligned} \dot{x}_i &= \mathbf{A}_i x_i + \mathbf{B}_i u_i, \\ y_i &= \mathbf{C}_i x_i, \qquad i=1,2, \ldots, N, \end{aligned} \tag{3-4}$$

where $x_i \in R^{n_i}, y_i \in R^q$, y $u_i \in R^{m_i}$ are the state vectors, output, and control input, respectively.

By definition, output consensus for heterogeneous systems, defined by (3-4), is achieved if, for any initial conditions, the follow condition is fulfilled

$$\lim_{t\to\infty} \|y_i - y_j\| = 0, \quad \forall \text{ i, j=1, 2, ..., N.}$$

For a multi-agent system, output feedback control design problem can be described by the follow equation [42]

$$\begin{aligned} \dot{\zeta}^i &= \mathbf{F}^i \zeta^i + \mathbf{G}_1^i y^i + \mathbf{G}_2^i v^i. \qquad i=1, \ldots, N. \\ u^i &= \mathbf{H}^i \zeta^i + \mathbf{J}_1^i y^i + \mathbf{J}_2^i v^i, \end{aligned}$$

where $\zeta^i \in \mathbb{R}^{p^i}$, $v^i = \sum_{j\in N_i} \alpha_{ij}(y^j - y^i) = -\sum_{j\in N} l_{ij} y^j$. The consensus definition implies the existence of a signal $\phi(t)$ such as $\lim_{t\to\infty} y^i(t) - \phi(t) = 0$ for all i. $\phi(t)$ is the consensus among the agents. Because the whole system is linear the synchronism signal $\phi(t)$ is required to be the linear system output described by $\dot{w} = Sw$ y $\phi = Rw$, where $\mathbb{R}^q$ and the couple (S, R) is observable.

3.2.2. Consensus for Distributed Systems with Delay

In a graph defined by $G = (V, E, A)$, the state for the discrete system and the consensus protocol law for directed and undirected graph is given by

$$x_i(k+1) = x_i(k) + u_i(k), \quad i \in \{1, \cdots, n\}$$
$$u_i(k) = \sum_{j \in N_i} a_{ij}(x_j(k) - x_j(k))$$

where $x_i(k) \in \mathbb{R}$, and $u_i(k) \in \mathbb{R}$ is the control input.

A distributed system is heterogeneous if it has different input delays. If each agent is subject to an input delay D_i, the distributed system can be written as [36]

$$x_i(k+1) = x_i(k) + u_i(k - D_i) \quad i \in \{1, \cdots, n\}$$

In a network in which each agent is subject to diverse communication delays, the delay between two agents is represented by τ_{ij} it means the delay from agent j to agent i. The consensus equation can be written as follows [36]

$$u_i(k) = \sum_{j \in N_i} a_{ij}(x_j(k - \tau_{ij}) - x_j(k))$$

The consensus is reached if $\lim_{k \to \infty} x_i(k) = c$, $\forall i \in \{1, \cdots, n\}$ where $c \in \mathbb{R}$ is a constant, then the closed loop system can be written as

$$x_i(k+1) = x_i(k) + \sum_{j \in N_i} a_{ij}(x_j(k - \tau_{ij} - Di) - x_i(k - D_i)) \quad i \in \{1, \cdot, n\}$$

3.2.3. Distributed PID Control

In [43], three protocol categories for clock synchronization are presented:

- *Tree-structure based:* In a tree-structure based a reference node is selected and a spanning tree rooted at this reference node is created.
- *Cluster-structure based:* at this approach, the network is divided into clusters, each one with a head node. Inside the cluster, each agent synchronizes with the head node, then each cluster head node synchronizes with the other head nodes. One of the major disadvantages of this approach is the neediness of rebuild the clusters in case of the head node is disconnected.
- *Fully distributed:* this approach allows to synchronize each agent without a complex communication system. Each agent synchronizes using local information from a set of

neighbors using consensus protocol. This way, scalability and plug and play capacity are improved.

Suppose a system defined by the next state equation set

$$\dot{x}(t) = \mathbf{A}x(t) + \mathbf{B}u(t) + d(t)$$
$$y(t) = \mathbf{C}x(t) + \eta(t),$$

A centralized PI control to made the error zero $r_i(t) - y_i(t) = e_i(t) = 0$ can be written as

$$u_i(t) = k_i^P e_i(t) + k_i^I \int_0^t e_i(\tau)d\tau$$

while a distributed PI-control can be written as follows [26]

$$\dot{z}_i(t) = e_i - \gamma \sum_{j \in N_i} c_{ij}(z_i(t) - z_j(t))$$
$$u_i(t) = k_i^P e_i(t) + k_i^I z_i(t)$$

In [44], an output synchronization linear multi-agent model with constant disturbances is proposed. This uses the integral action for a system defined by

$$\dot{x}_k = \mathbf{A}x_k + \mathbf{B}u_k + Pd_k$$
$$y_k = \mathbf{C}x_k,$$

with $d_k(t) \in \mathbb{R}^{n_d}$ is an external disturbance.

Defining the consensus as follow

$$\dot{\zeta}_k = \sum_{j=1}^{N} a_{kj}(y_j - y_k)$$

Theorem (1) from [44] proposed the follow control action

$$u_k = k_p \sum_{j=1}^{N} a_{kj}(x_j - x_k) + k_I \zeta_k$$

Several works study the control of frequency in synchronous generators and the model for transmission and distribution IEEE models, and distributed generators in a microgrid. In the next section, the distributed frequency control is presented.

3.2.4. Frequency Control of Power Systems

The use of renewable and distributed power generation and storage systems, raises the frequency fluctuations in utility systems and microgrids, creating the need for disturbance attenuation. In the first place, a proportional control is used to manage the frequency, but this is not able to reach asymptotically the reference [45], because of that, integral action is used.
In [26], a nonlinear consensus protocol for single and double integrator dynamics is proposed. The dynamics models are presented in (3-5)

$$\dot{x}_i = d_i + u_i \quad \text{Single Integrator} \qquad \begin{cases} \dot{x}_i = v_i \\ \dot{v}_i = d_i + u_i \end{cases} \quad \text{Double Integrator} \tag{3-5}$$

where d_i is a constant disturbance. Then, a distributed control for single-integrator action with damping is presented.

$$u_i = -\sum_{j \in N_i} \left(b(x_i - x_j) + \alpha \int_0^t (x_i(\tau) - x_j(\tau)) d\tau \right) - \delta(x_i - x_i(0))$$

where α and b are positive constants and $\delta \in \mathbb{R}^+$.

In [26], is presented a nonlinear consensus for agents with single and double-integrator dynamics, establishing the conditions for consensus in a static graph. It is demonstrated that agents reach asymptotic consensus when there are constant disturbances. Also, it is shown that *a decentralized PI control* for a large class of systems, is not a good control strategy.

In [46], a consensus for complex networks synchronization using a PI coupling is proposed. The linear coupling is extended to be used in networks with non-identical nodes or when it is affected by disturbances. Assuming a heterogeneous system of N agents

$$\dot{x}_i(t) = \rho_i x_i(t) + \delta_i + u_i(t) \qquad i=1,\ldots,\ N. \tag{3-6}$$

where $x_i(t) \in \mathbb{R}$ represents the state of the i-th agent, $\rho_i \in \mathbb{R}$ is the agent pole (a node uncoupled from the network can be either stable if $p_i < 0$ or unstable if $\rho_i < 0$). δ_i is a disturbance, and u_i is the control input. Agent pole and disturbances can be different for each agent.

The consensus manifold is defined by $S := \{x_j(t) - x_i(t)\} \quad \forall \quad i, j \in \{1, \cdots, N\}$. It is said that a group of N agents reach admissible consensus if $\lim_{t \to \infty} x_i(t) \in S_i$, the condition for the

control entry is that $\|u_i(t)\| < +\infty \quad \forall \quad i, j \in \{1, \cdots, N\}$. Additionally, the $\epsilon-$ admissible consensus can be defined if $\lim_{t\to\infty} x(t) \leq \epsilon$ for an arbitrary $\epsilon > 0$.

In [46] is proposed a distributed PI strategy (DPI) to achieve admissible consensus in a network of heterogeneous linear agents

$$u_i = -\sum_{j=1}^{N} \alpha l_{ij} x_{ij}(t) + z_i(t)$$

$$\dot{z}_i(t) = -\sum_{j=1}^{N} \beta l_{ij} x_j(t)$$

where $z_i(t) \in \mathbb{R}$ represents the state of the distributed integral action with $\alpha \geq 0$ and $\beta \geq 0$.

The DPI strategy is used to synchronized N droop-controlled inverters, demonstrating that the distributed integral action reduced the steady-state error effectively even with non-identical nodes. This consensus approach is useful to synchronize nodes with nonlinear dynamic.

In [47], a PID controller to reach consensus in networks of homogeneous and heterogeneous linear systems with constant disturbances is presented, convergence is demonstrated using Lyapunov functions. It presents the conditions that make the power network highly heterogeneous, such as error measurements, load variation, and communication failures.

The model for N nodes with heterogeneous first-order linear dynamics is given by expression (3-6). The PID consensus protocol for a network of N agents is

$$u_i(t) = -\sum_{j=1}^{N} L_{ij} \left[\alpha x_j(t) + \beta \int_0^t x_j(\tau) d\tau + \gamma \dot{x}_j(t) \right] \tag{3-7}$$

where L_{ij} is the Laplacian matrix, $\alpha \geq 0$, $\beta \geq 0$, and $\gamma \geq 0$.

In expression (3-7) consensus for proportional and integral terms has only one adjacency matrix represented by a unique Laplacian matrix. Same authors, propose in [48], and [49] a distributed control in which proportional and integral terms have different Laplacian matrices, this approach is called multilayer or multiplex PI control, and is used to achieve the consensus of heterogeneous agents. Based on system (3-6), the control strategy is given by

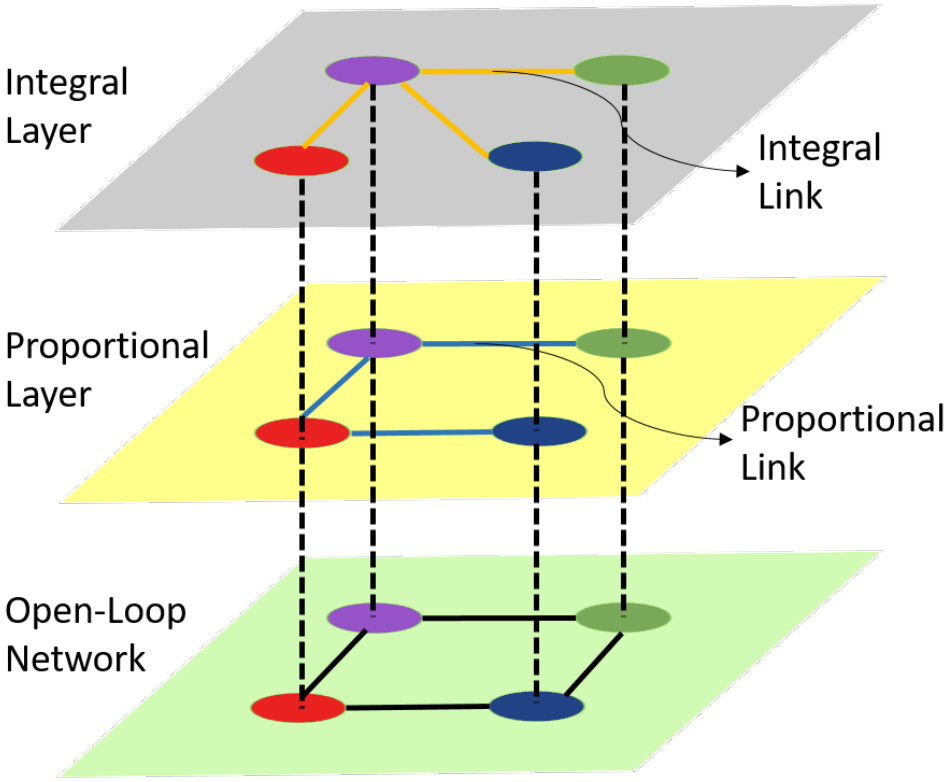

Figure 3-6.: Multiplex PI control representation [48]

$$u_i(t) = \sigma_P \sum_{j=1}^{N} \alpha_{ij}(x_j(t) - x_i(t)) + \sigma_I \sum_{j=1}^{N} \beta_{ij} \int_0^t (x_j(\tau) - x_i(\tau))d\tau \tag{3-8}$$

where σ_P, and σ_I are the constant gain factors for proportional and integral terms, respectively. α_{ij} represents the ij term of the proportional adjacency matrix, while β_{ij} is the term for integral term. (3-8) is represented graphically by several layers over the physical system as it is shown in Figure **3-6**.

3.2.5. Factors to Consider for a Microgrid and a Cluster

Several aspects can define the behavior of the agents (inverters and microgrids) in a microgrid system, making them non-identical to the others. Inverters can have different frequencies of cut in the low-pass filters, different control gains, and transmission lines values. The same case is presented for a cluster of microgrids. Figure **3-7** summarize the principal aspects that make the agents non-identical to the others

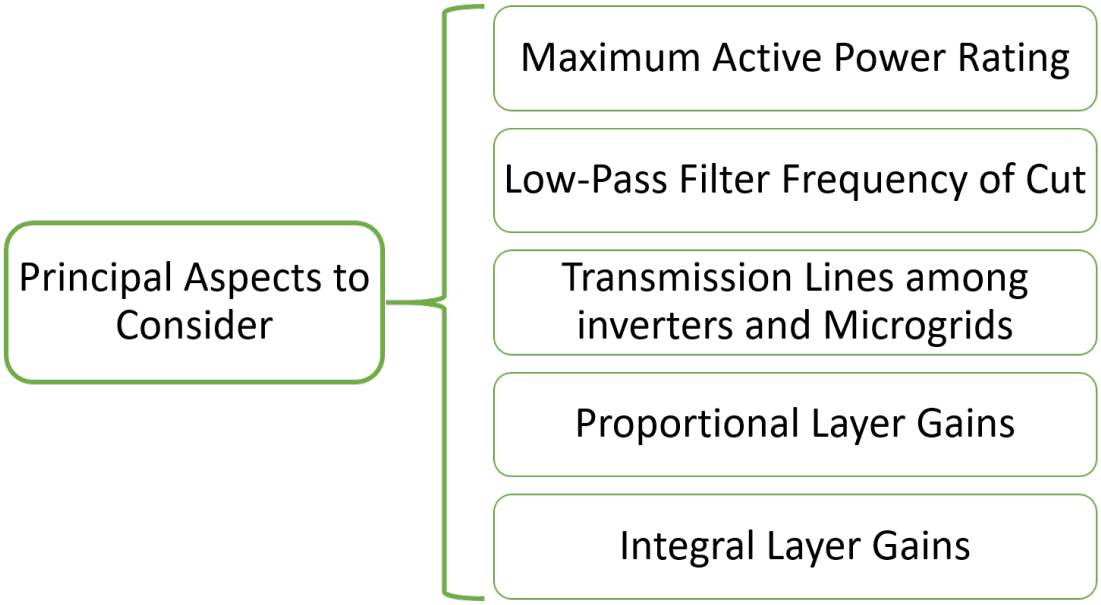

Figure 3-7.: Principal factors that make non-identical agents

3.3. Inverter and Cluster Modeling

Inverter and cluster are modeled following the same principle, the physical connection among agents are represented by undirected graphs. The active power flow from node i to node k in a network of n nodes is given by the following equation [50]:

$$P_{i,k} = G_{ik}V_i^2 - V_iV_k(G_{ik}\cos(\theta_{ik}) + B_{ik}\sin(\theta_{ik})),$$

where $P_{i,k} : \mathbb{S}^2 \times \mathbb{R}^2_{>0} \to \mathbb{R}$
Then, all the total injections of active power at node i is given by

$$P_i = G_{ii}V_i^2 - \sum_{k\in N_i} V_iV_k(G_{ik}\cos(\theta_{ik}) + B_{ik}\sin(\theta_{ik})),$$

with

$$G_{ii} = \hat{G}_{ii} + \sum_{k\in N_i} G_{ik}$$

where $\hat{G}_{ii}$ is the shunt conductance at node i.

For a lossless network (or predominantly inductive) the last equation can be simplified as follows

$$P_{e,i} = \sum_{j=1}^{n} E_iE_j|Y_{ij}|\sin(\theta_i - \theta_j). \tag{3-9}$$

where Y_{ij} corresponds to the admittance matrix, E_i and E_j are the voltages at nodes i, j respectively, and θ_i and θ_j are the phase voltage angles.

Phase differences between generator and common bus can be considered small enough to apply the mathematical expression $\sin\theta \approx \theta$, then (3-9) can be simplified as

$$P_{e,i} = \sum_{j=1}^{n} E_i E_j |Y_{ij}|(\theta_i - \theta_j). \tag{3-10}$$

The inverter is modeled as a controlled voltage source connected through an inductive transmission line. A set of n inverters in an isolated microgrid can be represented by a weighted graph $G(V, E, A)$, where the set of nodes V is partitioned in $V = (V_L, V_I)$ corresponding to loads and inverters. At this model a voltage signal is assigned to each inverter as $E_i(t) = E_i \cos(\omega_{ref} t + \theta_i)$, (for more details see [51]) where ω_{ref} is the angular frequency reference, E_i is the voltage amplitude, and θ is the voltage phase angle. Following the same approach, the magnitude of the *voltage is considered constant* and fixed at every bus.

The equation model for the active power demanded by the loads is given by the follow expression

$$0 = P_i^* - \sum_{j=1}^{n} E_i E_j |Y_{ij}|(\theta_i - \theta_j). \quad i \in V_L$$

The power at the inverter i is determined by its physical connection with the others, this can be represented by a graph with and associated Laplacian matrix in which each generator is a node, and the weighted edges are given by (3-11):

$$\omega_{ij} = E_i E_j |Yij| \qquad P_{e,i} = \sum_{j=1}^{n} \omega_{ij}(\theta_i - \theta_j). \tag{3-11}$$

Based on droop equation the set of equations for N linearized inverters is given by

$$\dot{\theta}_i(t) = P_i^* - P_i(t) + u_i(t) \quad i \in 1, \cdots, N$$
$$P_i(t) = P_i^* - \sum_{j=1, j\neq i}^{N} E_i E_j |Y_{ij}|(\theta_i - \theta_j)$$

where θ_i is the phase of each inverter, $u_i(t)$ is the exogenous control signal.

The *droop-phase control* is a decentralized paradigm that allows achieving power sharing without change significantly the frequency of the system. The phase for inverter i is given by the follow expression

$$\theta_i = \theta_{ref} - m_i(P_{ref} - P_i) \tag{3-12}$$

where θ_{ref} is the phase reference value, m_i is the droop-phase gain in $rads$, and $Pref$ and P_i represent the reference and measure active power values, respectively. Assuming that all the agents are synchronized at $t > 0$, the angle reference parameter can be set at zero ($\theta_{ref} = 0$), and the active power reference can be chosen zero too, simplifying (3-12).

$$\theta_i = m_i P_i \tag{3-13}$$

The droop-phase gain can be selected according to

$$m_i = \frac{\Delta f}{P_{max}} \qquad\qquad m_i = \frac{0{,}1}{P_{max}} \tag{3-14}$$

For a **droop-free system**, small phase variations are introduced directly at the phase angle at each inverter. The voltage at inverter i is given by the follow expression

$$V_i(t) = E_i(\omega_{ref} t + \theta_i)$$

Then, as each inverter achieves its frequency of reference ω_{ref}, the microgrid power sharing and synchronization problem can be studied as an equilibrium problem in which all the inverters are in rotating frame. Additionally, the set of angle variations θ is restrained to the interval $\gamma \in [0, \pi/2]$. The phase angle for inverter i can be written as

$$\dot{\theta}_i = u_i$$

$$u_i = c \sum_{i \in N_i}^{N} a_{ij}(P_j - P_i)$$

According to [34] this equation can be written in a matrix form as

$$\dot{\theta} = -c\mathbf{L}\mathbf{P}$$

where $\mathbf{P}$ is the matrix representation of the power at each inverter and $\mathbf{L}$ is the Laplacian matrix of the communication graph for the whole network.

As the active power at each inverter is normalized according to its maximum active power rating, a new constant can be defined as follows

$$k_i = \frac{1}{P_{max,i}}$$

The instantaneous active power $p(t)$ is measured and then pass through a low-pass filter to get a medium value, the frequency of cut of this filter is smaller than one of the voltage and current controllers [18].

$$P_i = p_i \frac{\omega_{c,i}}{s + \omega_{c,i}}$$

$$P_i = p_i \frac{1}{\tau_i s + 1}$$

where τ_i is the constant time for the filter i and P_i is the filtered active power.
This equation can be rewritten to get an expression in time domain

$$P_i \tau_i s + P_i = p_i$$

$$\tau_i \dot{P}_i = -P_i + p_i$$

Power Sharing Condition: The system must be capable to guaranty the power sharing condition among the inverters, fulfilling the next expression

$$\frac{P_i}{P_{max,i}} = \frac{P_j}{P_{max,j}} \quad \forall \quad i, j \in N \tag{3-15}$$

The distributed PI strategy or DPI is expressed in the follow equations

$$\dot{\theta}_i = u_i \tag{3-16}$$

$$u_i = \alpha \sum_{j \in N_i}^{N} a_{ij}(k_j P_j - k_i P_i) + z_i$$

$$\dot{z}_i = \beta \sum_{j \in N_i}^{N} b_{ij}(k_j P_j - k_i P_i)$$

$$\dot{P}_i = \tau_i^{-1} k_i \sum_{j=1}^{n} E_i E_j |Y_{ij}|(\theta_i - \theta_j)] - \tau_i^{-1} P_i$$

where $\alpha, \beta \in \mathbb{R} > 0$ represent the constant gain value for the proportional and integral consensus expression. a_{ij} and b_{ij} are the corresponding terms from proportional and integral adjacency matrices, and τ_i is the time constant for the i-th active power filter.
Defining $\mathbf{K}$ as the matrix whose diagonal is the set of constant k_i. The set of time values for the low-pass filters is represented by the diagonal matrix $\mathbf{T}$, and $\mathbf{P}$ is the vector that contains the instantaneous active power measures at each inverter.

$$\mathbf{K} = \begin{pmatrix} k_{11} & 0 & \cdots & 0 & 0 \\ 0 & k_{22} & \cdots & 0 & 0 \\ 0 & 0 & \ddots & 0 & 0 \\ \vdots & \cdots & \cdots & \vdots & \vdots \\ 0 & 0 & 0 & 0 & k_{nn} \end{pmatrix}; \quad \mathbf{T} = \begin{pmatrix} \tau_{11}^{-1} & 0 & \cdots & 0 & 0 \\ 0 & \tau_{22}^{-1} & \cdots & 0 & 0 \\ 0 & 0 & \ddots & 0 & 0 \\ \vdots & \cdots & \cdots & \vdots & \vdots \\ 0 & 0 & 0 & 0 & \tau_{nn}^{-1} \end{pmatrix}; \quad \mathbf{P} = \begin{pmatrix} P_1 \\ P_2 \\ \vdots \\ P_n \end{pmatrix}.$$

The complete closed-loop system (3-16) can be written in a matrix form as

$$\begin{aligned} \dot{\theta} &= -\alpha \mathbf{L_p K P} + \mathbf{Z} \\ \dot{\mathbf{Z}} &= -\beta \mathbf{L_I K P} \\ \dot{\mathbf{P}} &= \mathbf{T K L_c} \theta - \mathbf{T P} \end{aligned} \tag{3-17}$$

where $\mathbf{L_p}$, $\mathbf{L_I}$, and $\mathbf{L_c}$ are the Laplacian matrices for the proportional, integral, and physical connection terms, respectively.

System (3-17) is represented by Figure **3-8**, notice that the entry is the phase value, and the output is the active power. The closed-loop phase control system represented by $\mathbf{A}$ must ensure that is locally exponentially stable, and the power sharing condition is guaranteed.

$$\begin{bmatrix} \dot{\theta} \\ \dot{Z} \\ \dot{P} \end{bmatrix} = \begin{bmatrix} 0_{N\times N} & 1_{N\times N} & -\alpha L_p K \\ 0_{N\times N} & 0_{N\times N} & -\beta L_I K \\ T K L_c & 0_{N\times N} & -T \end{bmatrix} \begin{bmatrix} \theta \\ Z \\ P \end{bmatrix} \tag{3-18}$$

Let (θ^*, Z^*, P^*) be the equilibrium of (3-17), satisfying the following equations

$$\begin{aligned} -\alpha \mathbf{L_p K P}^* + \mathbf{Z}^* &= 0_{N\times 1} \\ -\beta \mathbf{L_I K P}^* &= 0_{N\times 1} \\ \mathbf{T K L_c} \theta^* - \mathbf{T P}^* &= 0_{N\times 1} \end{aligned} \tag{3-19}$$

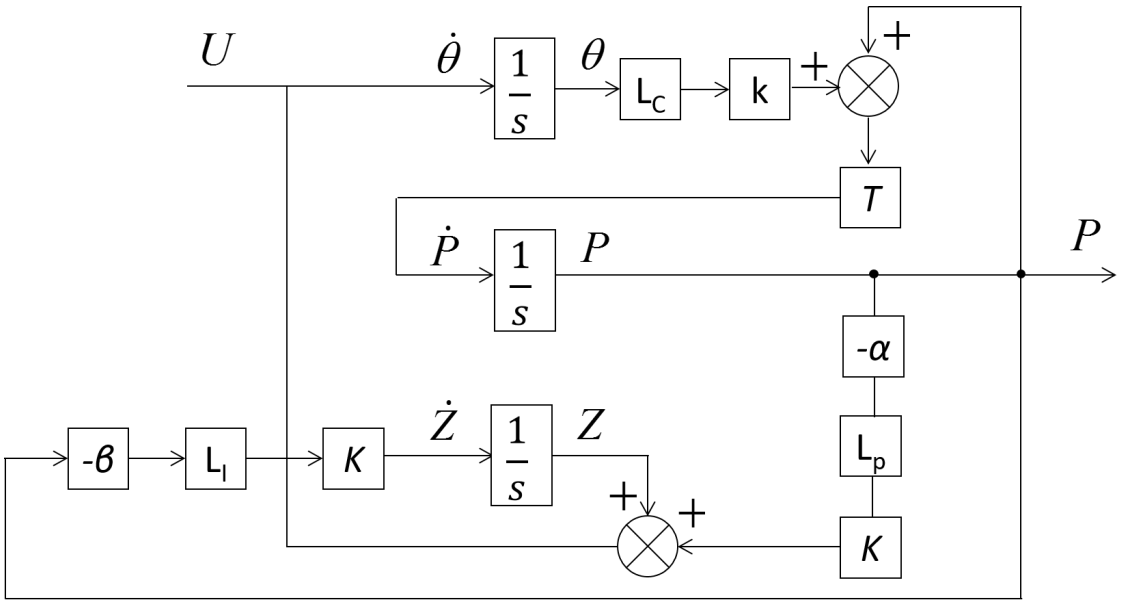

Figure 3-8.: Block diagram of system (3-17)

From the second equation of (3-19) it can be inferred that $\mathbf{P}^* = \beta 1_{1\times N}$, then the first equation of (3-19) becomes $\mathbf{Z} = -\alpha \mathbf{L}_p \mathbf{K} \mathbf{P}^* = (-\alpha \mathbf{L}_p \mathbf{K})(\beta \mathbf{1}_{1\times N}) = \mathbf{0}$, which means that the contribution of integral term tends to zero, once all the values of vector $\mathbf{P}$ are the same, this fulfill condition (3-15) which guaranty the power sharing condition when $\frac{P_i}{P_{max,i}} = \frac{P_j}{P_{max,j}}$, from the third equation it can be seen that the active power vector depends of the $\mathbf{L_c}$ values, and the vector of phase differences θ.

Finding the characteristic equation of system (3-18), as $0 = |s\mathbf{I} - \mathbf{A}|$ as follows

$$|s\mathbf{I} - \mathbf{A}| = \left| \begin{bmatrix} s & 0 & 0 \\ 0 & s & 0 \\ 0 & 0 & s \end{bmatrix} - \begin{bmatrix} 0_{N\times N} & 1_{N\times N} & -\alpha L_p K \\ 0_{N\times N} & 0_{N\times N} & -\beta L_I K \\ TKL_c & 0_{N\times N} & -T \end{bmatrix} \right| = \left| \begin{bmatrix} s & -1_{N\times N} & \alpha L_p K \\ 0_{N\times N} & s & \beta L_I K \\ -TKL_c & 0_{N\times N} & s+T \end{bmatrix} \right|$$

$$|s\mathbf{I} - \mathbf{A}| = s^3 + Ts^2 + TKL_c \alpha L_p K s + \beta L_I K T K L_c$$

The Laplacian matrices $\mathbf{L_c}$, $\mathbf{L_p}$, and $\mathbf{L_I}$ are positive-definite. Matrices $\mathbf{T}$ and $\mathbf{K}$ are diagonal matrices and positive definite (positive semi-definite) matrices too, if all $a_{ij} \geq 0$. The product of a positive definite matrix and a symmetric matrix is positive definite too.
As the eigenvalues of Laplacian matrices $\mathbf{L}_I$, $\mathbf{L}_p$, and $\mathbf{L}_c$ are positive ($\lambda_{p,i} \geq 0$, $\lambda_{I,i} \geq 0$, $\lambda_{c,i} \geq 0$). The characteristic polynomial can be written as

$$0 = s^3 + bs^2 + c\lambda_{c,i}\lambda_{p,i}s + d\lambda_{I,i}\lambda_{c,i} \tag{3-20}$$

Characteristic Equation (3-20) solutions are in the left half of the complex plane ($s \in \mathbb{C}^-$) if and only coefficients are positive $b > 0$, $c > 0$, and $d > 0$ according to the Routh-Hurwitz stability criterion.

3.3.1. Cluster Modeling

Several microgrids are interconnected through transmission lines forming a cluster, the dynamic of each microgrid is described by the sum of the inverters contribution. As Figure **3-9** shows, the active power flows are shared among the microgrids, and the control actions are calculated using the communication network for the system.

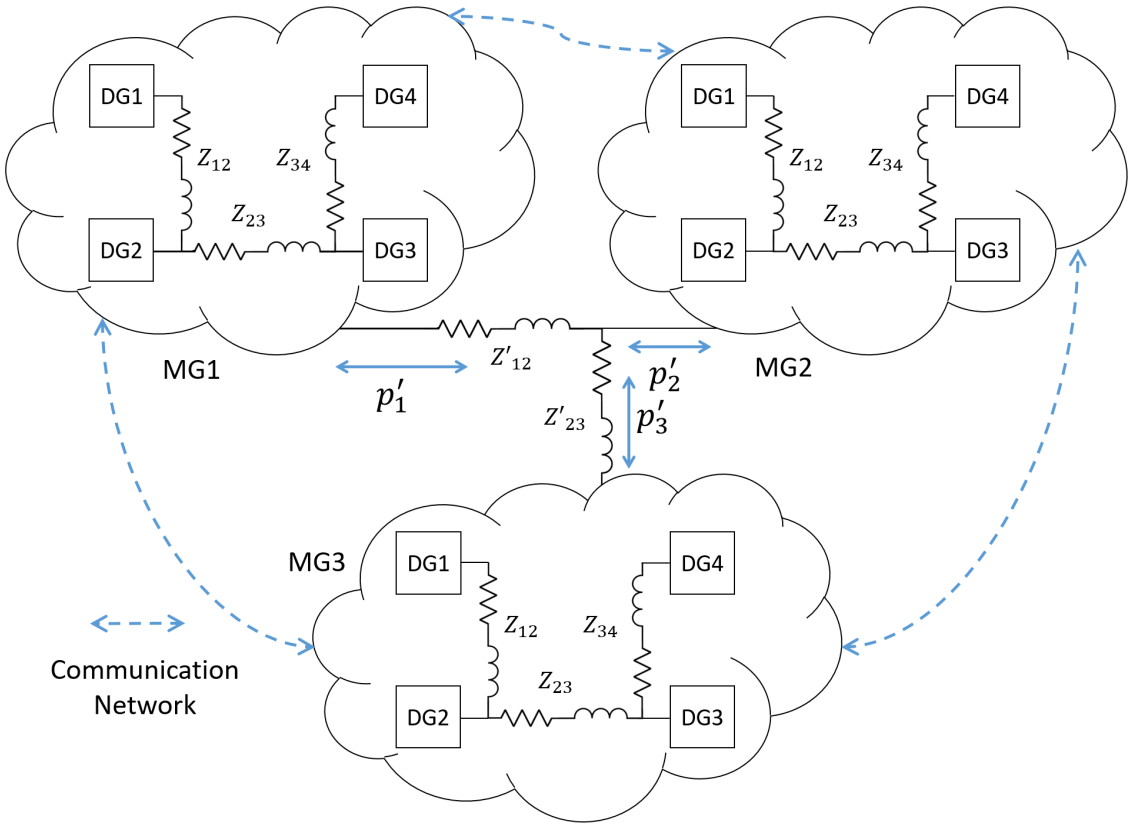

Figure 3-9.: Microgrid cluster

Based on the voltage equation for inverter i, the hierarchical control terms can be written as follows

$$V_i(t) = V_{max} \sin\left(\omega_{ref} t + \theta + \delta\right),$$

where θ is the local term from inverters, and δ is the global term from microgrids. Each term can be managed separately from the other if the frequency of cut of their low pass filters

are different and the response of the controller for the microgrids is slower than the response of the controller for the inverters. Global and local phase terms are managed separately, considering that the reference values of the controller are equal to zero.

If the active power injected for a single inverter is given by (3-10), in a similar form, the active power injected for microgrid k is given by the following expression

$$P_{e,k} = \sum_{k=1}^{m} E_k E_l |Y_{kl}|(\delta_k - \delta_l).$$

The phase term from microgrid is generated based on the active power injections among microgrids. First, the maximum active power for each microgrid is calculated adding the maximum active power rating of each inverter inside the microgrid, then, the maximum active power at microgrid k is equal to the sum of the maximum active power at inverter i

$$P_{max,k} = \sum_{i=1}^{N} P_{max,i}.$$

The active power is measured at the PCC of each microgrid, then is normalized according to its maximum active power rating, this value is filtered through a low-pass filter with a cut frequency lower than the inverter controller. These values are compared with the consensus equation and integrated to obtain the phase term. Notice that each microgrid shares active power through its coupling transform, as is shown in Figure **3-10**, not additional control is necessary because the *predominantly inductive line* condition is fulfilled.

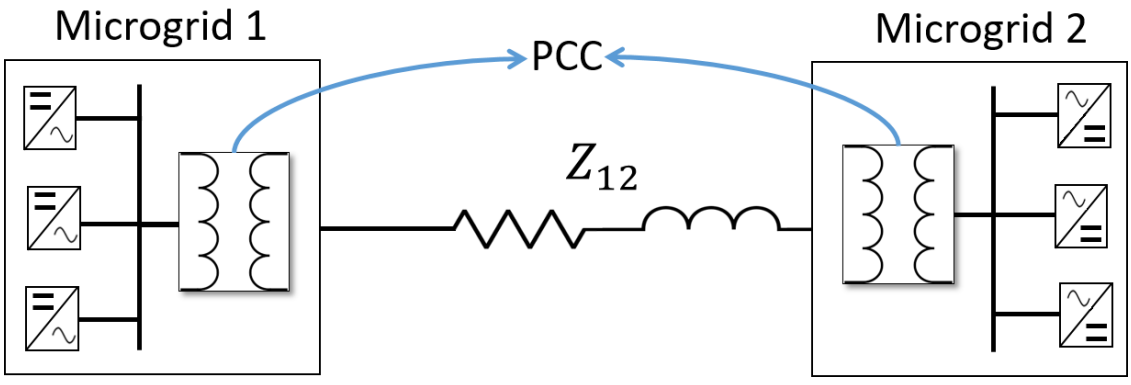

Figure 3-10.: Connection among microgrids through the PCC

The phase angle for microgrid k can be written as

$$\dot{\delta}_k = u_k$$

$$u_k = -c \sum_{l \in N_k}^{m} b_{kl}(P_l - P_k)$$

The active power constant for microgrid k is given by the following expression

$$d_k = \frac{1}{P_{max,k}}$$

then the phase term for the microgrid cluster can be written as

$$\dot{\delta}_k = c \sum_{l \in N_k}^{M} b_{kl}(d_l p_l - d_k p_k)$$

Similarly to the local controller, the active power measured at each microgrid is filtered through a low-pass first order filter. The differential equation including the time constant for microgrid k is given below

$$\tau_k \dot{P}_k + P_k = P_{e,k}$$

$$\dot{P}_k = \tau_k^{-1} \sum_{k=1}^{m} E_k E_l |Y_{kl}|(\delta_k - \delta_l) - \tau_k^{-1} P_k$$

Defining the D matrix as a diagonal matrix whose diagonal is the d_k values

$$\mathbf{D} = \begin{pmatrix} d_{11} & 0 & \cdots & 0 & 0 \\ 0 & d_{22} & \cdots & 0 & 0 \\ 0 & 0 & \ddots & 0 & 0 \\ \vdots & \cdots & \cdots & \vdots & \vdots \\ 0 & 0 & 0 & 0 & d_{nn} \end{pmatrix}; \qquad \mathbf{T} = \begin{pmatrix} \frac{1}{\tau_{11}} & 0 & \cdots & 0 & 0 \\ 0 & \frac{1}{\tau_{22}} & \cdots & 0 & 0 \\ 0 & 0 & \ddots & 0 & 0 \\ \vdots & \cdots & \cdots & \vdots & \vdots \\ 0 & 0 & 0 & 0 & \frac{1}{\tau_{nn}} \end{pmatrix};$$

Then, the system equations can be written in a matrix form as

$$\dot{\mathbf{\Delta}} = -c\mathbf{L_g}\mathbf{D}\mathbf{P} \qquad \dot{\mathbf{P}} = \mathbf{T}\mathbf{L}_\mathbf{c}^{'}\mathbf{\Delta} - \mathbf{T}\mathbf{P},$$

where $\mathbf{\Delta}$ is the matrix representation for δ_k, $\mathbf{L_g}$ is the Laplacian matrix for the global connection among microgrids, and $\mathbf{L}_\mathbf{c}^{'}$ is the weighted matrix representing the physical connection

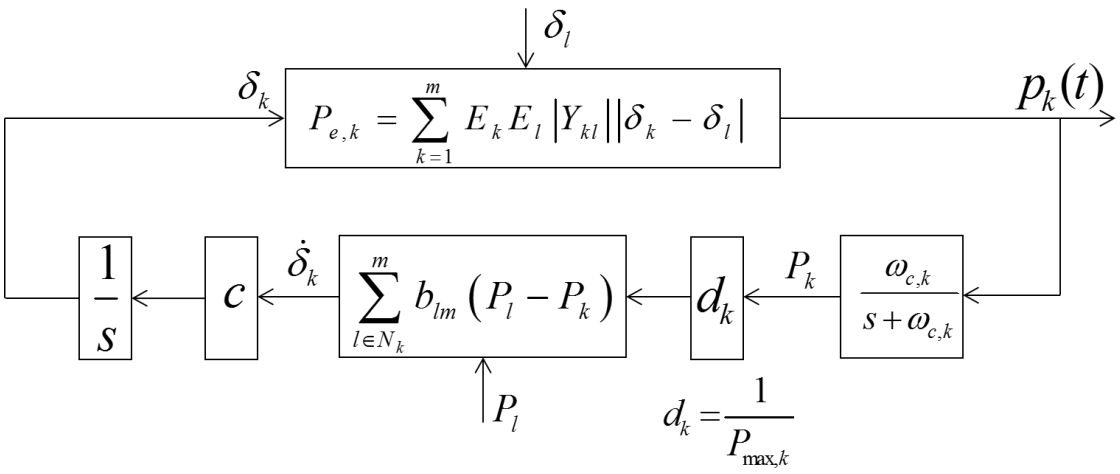

Figure 3-11.: Block diagram control

among the microgrids. Figure **3-11** shows the control strategy for the $k-th$ microgrid of the cluster, in this case only integral action is taking into account.

$$\begin{bmatrix} \dot{\Delta} \\ \dot{P} \end{bmatrix} = \begin{bmatrix} 0 & -cL_gD \\ TL_c' & -T \end{bmatrix} \begin{bmatrix} \Delta \\ P \end{bmatrix} \tag{3-21}$$

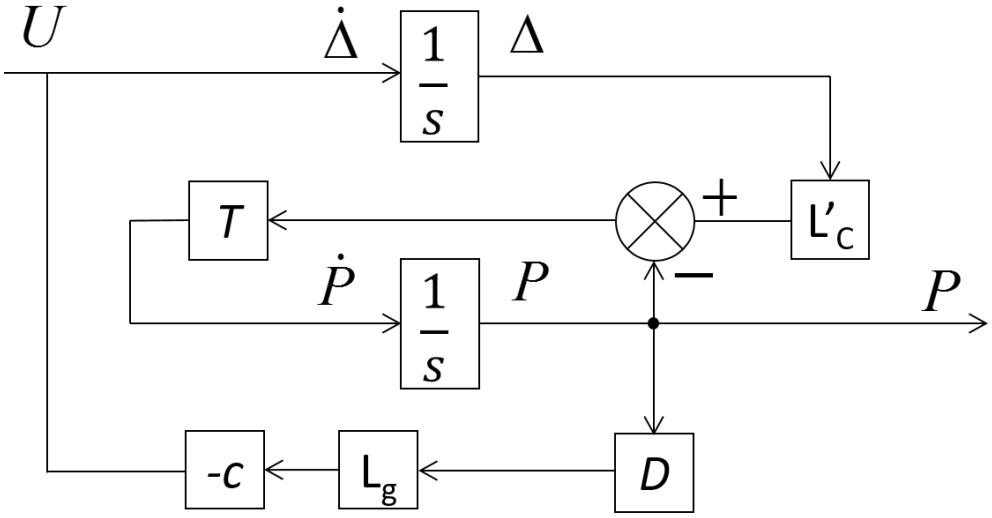

Figure 3-12.: Block diagram for the microgrid global control

Figure **3-12** shows the block diagram control for the networked system, where T, L_c', L_g, Δ, P and D are the matrix representation. The constant value c is the consensus gain value. The eigenvalues of the close-loop system (3-21), are calculated making $|s\mathbf{I} - \mathbf{A}| = 0$, as follows

$$|s\mathbf{I}-\mathbf{A}| = \left| \begin{bmatrix} s & 0 \\ 0 & s \end{bmatrix} - \begin{bmatrix} 0 & -cL_gD \\ TL_c^{'} & T \end{bmatrix} \right| = \left| \begin{bmatrix} s & cL_gD \\ -TL_c^{'} & s+T \end{bmatrix} \right|$$

Then, the characteristic polynomial with eigenvalues of the Laplacian matrices $\mathbf{L}_g$ and $\mathbf{L}_c^{'}$ given by ($\lambda_{g,i} \geq 0$, $\lambda_{c,i} \geq 0$) can be written as $0 = s^2 + Ts + TL_c^{'}cL_gD$, and in a general form

$$0 = s^2 + bs + c\lambda_{c,i}\lambda_{g,i} \tag{3-22}$$

The matrices $\mathbf{L_c^{'}}$, $\mathbf{L_g}$, $\mathbf{T}$, and $\mathbf{D}$ are positive definite (positive semi-definite). The coefficients of the characteristic polynomial (3-22) are positive $b > 0$ and $c > 0$ and fulfill the Routh-Hurwitz criterion. Then, the solutions are in the left half of the complex plane ($s \in \mathbb{C}^-$).

3.3.2. Graph Laplacian Potential

Graph Laplacian Potential allows determining the stability of multi-agent distributed system based on the 'potential energy' stored in a graph. The global system distributed control for microgrid k is represented by

$$\dot{\phi}_k = c \sum_{l \in N_k}^{m} b_{kl}(P_l - P_k)$$

In matrix form

$$\dot{\mathbf{\Phi}} = -c\mathbf{L_g}\mathbf{P_g},$$

where $\mathbf{P_g}$ represents the vector of active power values after being filtered by a low-pass filter and divide it for the maximum active power value. If the k-th value of normalized vector $\mathbf{P}$ remains bounded as $0 \leq P \leq 1$, based on expression (3-2), the next Lyapunov function is presented

$$\mathbf{V} = \sum_{k=1}^{m} p_k^2 = \mathbf{P_g}^\top \mathbf{P_g}.$$

This Lyapunov function is zero for $\mathbf{P_g} = \mathbf{0}$ and is positive definite. The time derivative of the Lyapunov-candidate function $\mathbf{V}$ along the trajectories is given by

$$\dot{\mathbf{V}} = 2\mathbf{P_g}^\top \dot{\mathbf{P}}_\mathbf{g}$$

Replacing the matrix expression for consensus at $\dot{\mathbf{P}}_\mathbf{g}$ equation becomes

$$\dot{\mathbf{V}} = 2\mathbf{P_g}^\top (-c\mathbf{L_g}\mathbf{P_g})$$

As the Lyapunov function is positive definite, and it is $\dot{\mathbf{V}}$ negative semidefinite along the trajectories, based on the LaSalle's invariance principle, and if the graph has a spanning tree, the trajectories tend to zero at steady state and the consensus is reached [52].

The same analysis can be used for the local controller of inverters. The local consensus expression and its matrix form is given by

$$\dot{\phi}_i = b \sum_{i \in N_i}^{N} a_{ij}(P_j - P_i)$$

$$\dot{\mathbf{\Phi}} = -b\mathbf{L_l}\mathbf{P_l}$$

The local Lyapunov function is given by

$$\mathbf{V} = \sum_{i=1}^{N} p_i^2 = \mathbf{P_l}^\top \mathbf{P_l}.$$

The time derivative of the Lyapunov-candidate function $\mathbf{V}$ along the trajectories is given by

$$\dot{\mathbf{V}} = 2\mathbf{P_l}^\top \dot{\mathbf{P}}_\mathbf{l}$$

Replacing the matrix expression for consensus at $\dot{\mathbf{P}}_\mathbf{l}$ equation becomes

$$\dot{\mathbf{V}} = 2\mathbf{P_l}^\top (-c\mathbf{L_l}\mathbf{P_l})$$

Functions $\mathbf{V}$ and $\dot{\mathbf{V}}$ fulfilled the requirements to be a Lyapunov function and its first derivative. If the system has a spanning tree, the trajectories tend to zero at steady state, and the consensus is reached.

4. Networked Microgrids

Several microgrids share power through a transmission line, and data using a communication system. As a first step, a single microgrid formed by several distributed energy resources is simulated using the droop-free approach. Second, a system of networked microgrids is presented using identical agents and compared with other based on heterogeneous agents. Based on the droop-free control paradigm presented in section 2. The control for a single microgrid is implemented as follows.

4.1. Distributed Control for a Single Microgrid

An inverter based microgrid with four DERs, each one with a virtual impedance loop to guarantee the predominantly inductive transmission line condition is simulated. The inverters are connected through transmission lines in a structure as it is shown in Figure 4.1

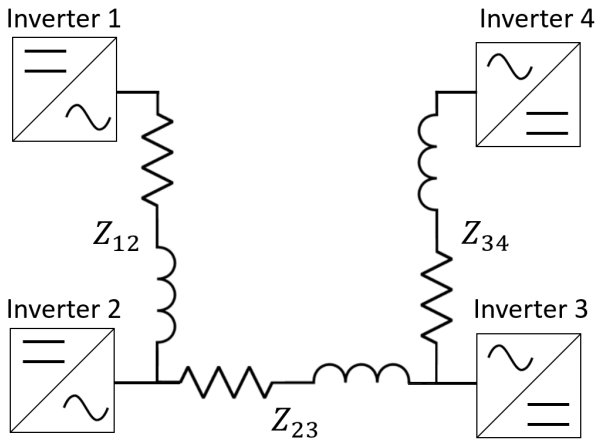

Figure 4-1.: Physical connection among inverters

First, a distributed PI control paradigm is used to synchronized and achieved power sharing among the inverters. The communication graph can be either the same of the physical connection or adopt different topologies, always with a spanning tree.

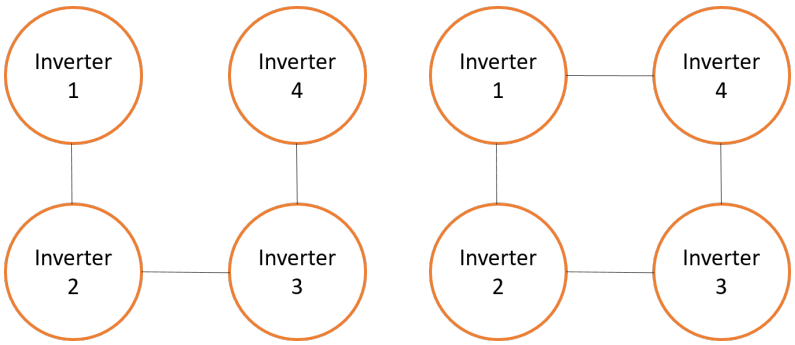

Figure 4-2.: Different graph topologies (Left.Case 1. Center. Case 2.)

$$d_{T1} = \begin{pmatrix} 1 & 0 & 0 & 0 \\ 0 & 2 & 0 & 0 \\ 0 & 0 & 2 & 0 \\ 0 & 0 & 0 & 1 \end{pmatrix} \quad A_{T1} = \begin{pmatrix} 0 & 1 & 0 & 0 \\ 1 & 0 & 1 & 0 \\ 0 & 1 & 0 & 1 \\ 0 & 0 & 1 & 0 \end{pmatrix} \quad L_{T1} = \begin{pmatrix} 1 & -1 & 0 & 0 \\ -1 & 2 & -1 & 0 \\ 0 & -1 & 2 & -1 \\ 0 & 0 & -1 & 1 \end{pmatrix}$$

$$d_{T2} = \begin{pmatrix} 2 & 0 & 0 & 0 \\ 0 & 2 & 0 & 0 \\ 0 & 0 & 2 & 0 \\ 0 & 0 & 0 & 2 \end{pmatrix} \quad A_{T2} = \begin{pmatrix} 0 & 1 & 0 & 1 \\ 1 & 0 & 1 & 0 \\ 0 & 1 & 0 & 1 \\ 1 & 0 & 1 & 0 \end{pmatrix} \quad L_{T2} = \begin{pmatrix} 2 & -1 & 0 & -1 \\ -1 & 2 & -1 & 0 \\ 0 & -1 & 2 & -1 \\ -1 & 0 & -1 & 2 \end{pmatrix}$$

Inverter based microgrid is simulated for each using the physical topology presented in Figure 4.1, first for identical agents, and after for introducing some different values at each agent. The consensus among agents for proportional and integral parts are the same following the structure of the topologies presented before.

4.1.1. Identical Agents

Microgrid parameters are shown in Table **4-1**. The system is simulated for both graph topologies presented in Figure 4.2.

First Case

Figure **4-3**, shows the active power sharing among the inverters of a microgrid. Notice, that, even when the system parameters are identical, the power sharing is not achieved at the same time due the connection among the inverters. In this case, inverter 1 supplies a major power quantity when a load is connected.

Figure **4-4**, and Figure **4-5** show the phase variations for proportional and integral terms, respectively. Variations tend to zero at steady state when power sharing is achieved in a few

Table 4-1.: Microgrid Parameters for Identical Agents

Maximum Active Power at each Inverter	$P_{max,1} = 20kW$ $P_{max,2} = 20kW$ $P_{max,3} = 20kW$ $P_{max,4} = 20kW$
Transmission Line Impedances	$Z_{12} = 0{,}23\Omega + j0{,}12$ $Z_{23} = 0{,}23\Omega + j0{,}12$ $Z_{34} = 0{,}23\Omega + j0{,}12$
Load 1 and Load 2	10kW+3kVA
Filter Frequency of Cut	$fc = 5$Hz
Proportional Constant	$\alpha = 0{,}5$
Integral Constant	$\beta = 0{,}5$
Bus Voltage	V=120$Vrms$

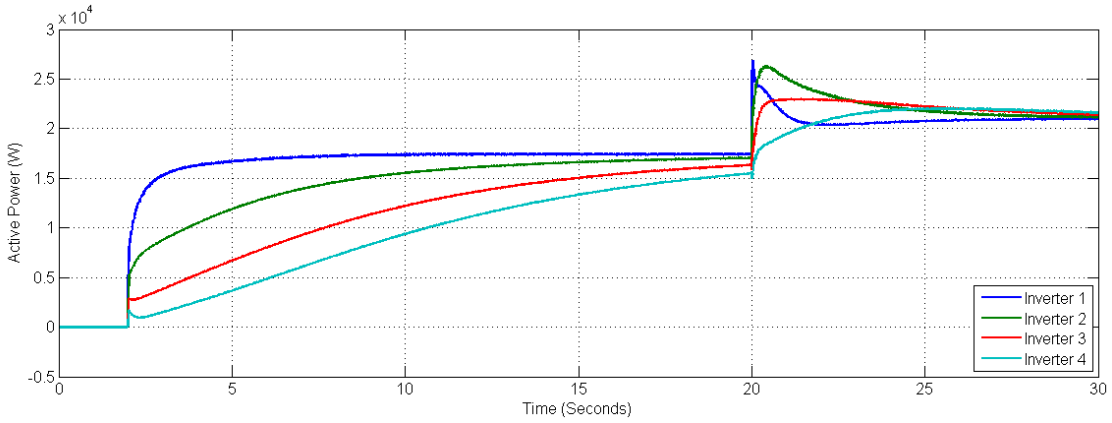

Figure 4-3.: Active power sharing among inverters case 1

seconds. At this case, phase variations and consensus behavior are identical because each adjacency matrix is connected with the topology of case 1.
Figure **4-6** shows the frequency variations for the microgrid measured at the common bus. The system achieves the frequency of reference after less than five seconds, and the variations are inferior to 0.2 Hz.

Second Case

Figure **4-7** shows the power sharing for case 2. Notice that in this case power sharing is achieved faster than in case 1. Proportional and integral consensus for the system in case 2 are shown in Figure **4-8**, and Figure **4-9**. In both cases, inverters achieved consensus faster than in case 1.

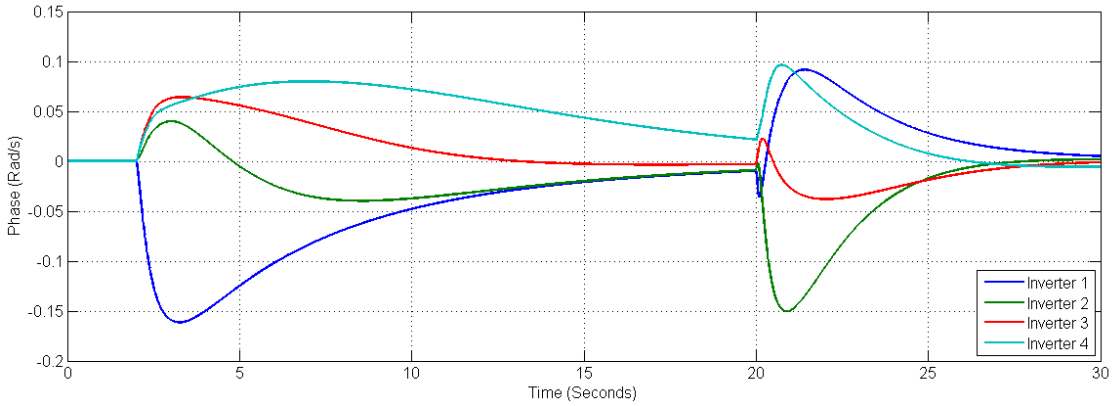

Figure 4-4.: Proportional term consensus among inverters case 1

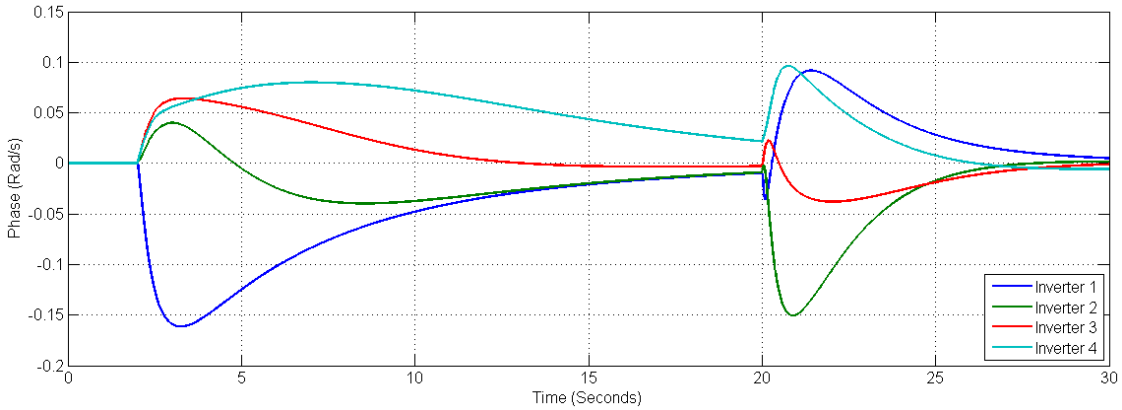

Figure 4-5.: Integral term consensus among inverters case 1

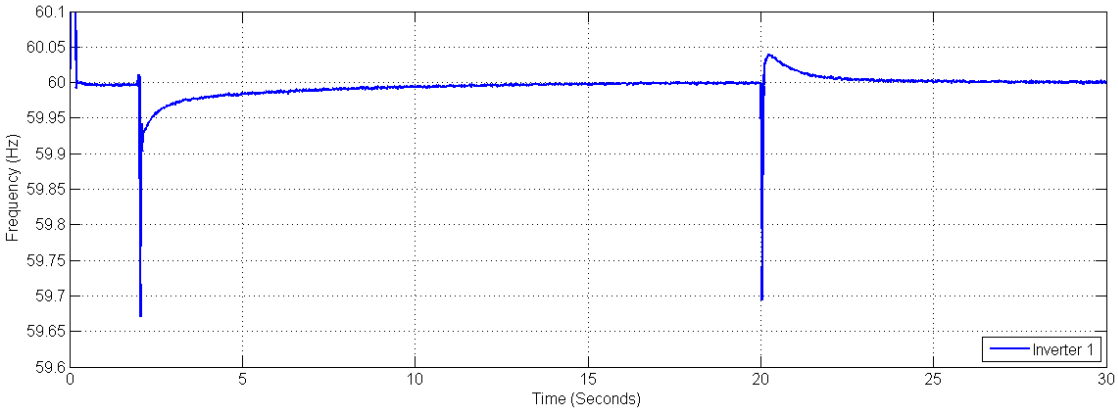

Figure 4-6.: Frequency of the system Case 1

Frequency variations of the systems last less than in case 1, as it is shown in Figure **4-10**.

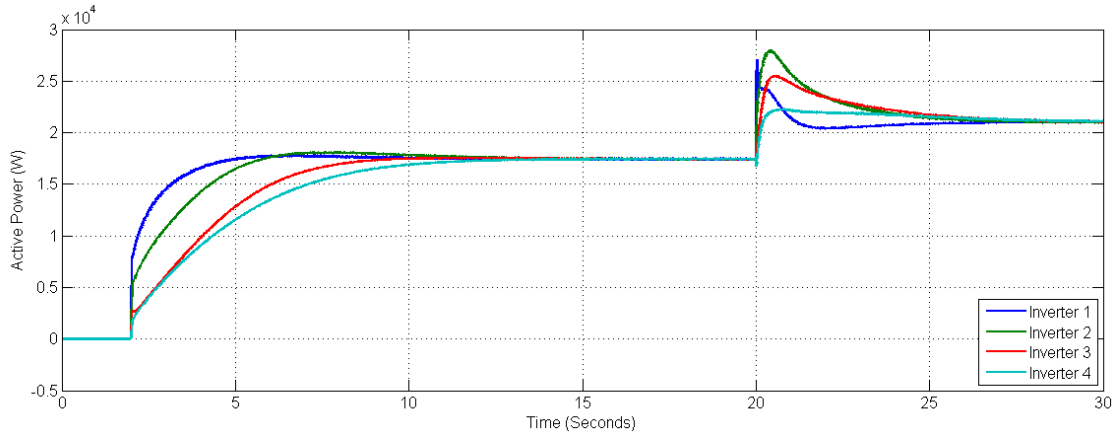

Figure 4-7.: Active power sharing among inverters case 2

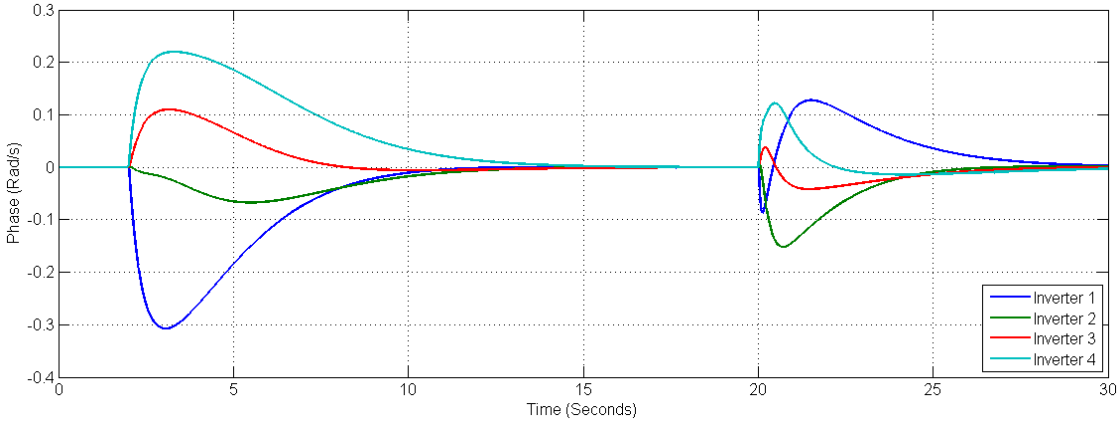

Figure 4-8.: Proportional term consensus among inverters case 2

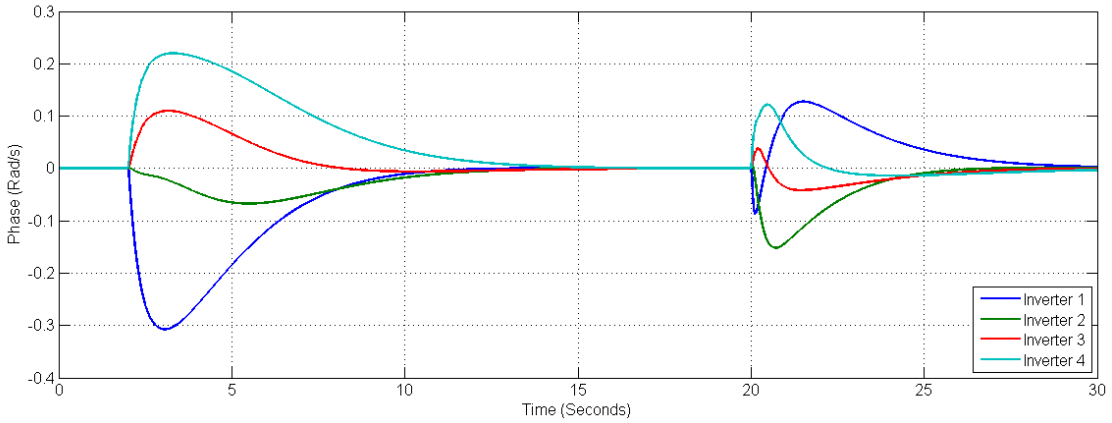

Figure 4-9.: Integral term consensus among inverters case 2

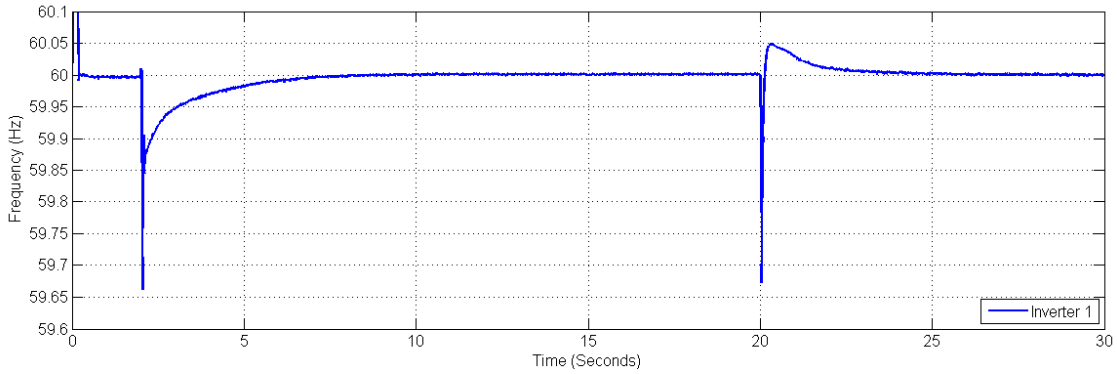

Figure 4-10.: Frequency of the system case 2

The overshot and the control response depend on the speed consensus variable, this is determined by the speed of the consensus constants α y β, and for the topology of the communication graph. For this case, the variable $\alpha = 0{,}5$ and $\beta = 0{,}5$ do not change the natural speed of the consensus given by the second eigenvalue of the Laplacian equation of the system.

Different Proportional and Integral Layers

At this case, different topologies are selected for the communication graph at proportional and integral layers. The effect is shown in the power sharing among agents at Figure **4-11**.

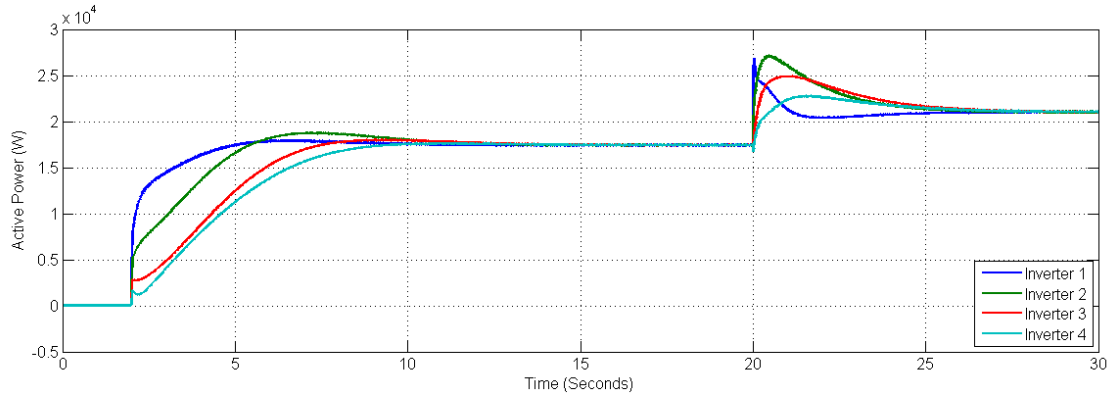

Figure 4-11.: Active power sharing among inverters different communication graphs

Figure **4-12** and Figure **4-13** show the consensus behavior for the proportional and integral terms, respectively. Each control layer can have a different communication topology, in this case, the proportional layer has the topology for case 1, while integral layer has the topology of case 2.

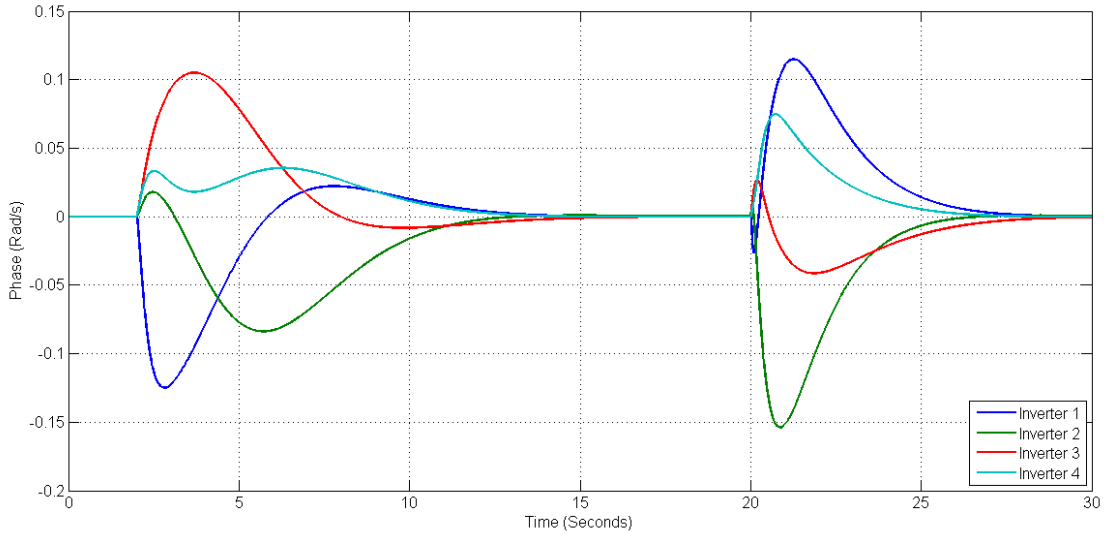

Figure 4-12.: Proportional term consensus among inverters topology of case 1

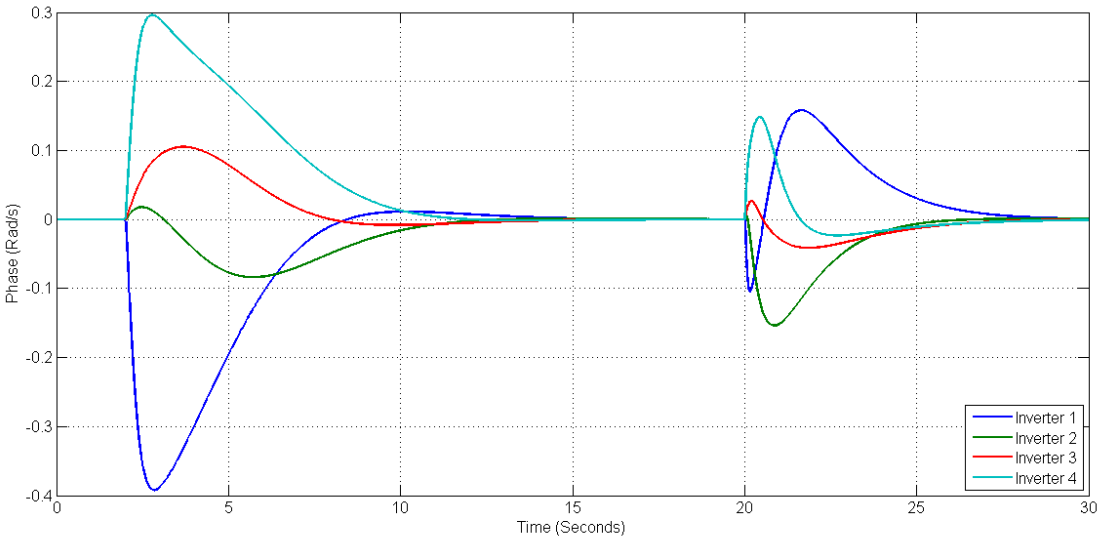

Figure 4-13.: Integral term consensus among inverters topology case 2

4.1.2. Non-Identical Agents

A microgrid is simulated following the same scheme than before, in this case, several differences are included: power capacities, frequencies of low pass-filters, proportional and integral gains, and transmission lines are different. Besides, two different charges are connected at $t = 2s$ and $t = 30s$, and the graph for proportional and integral layers are different, the proportional layer has the topology for case 1, while integral layer has the topology for case 2.

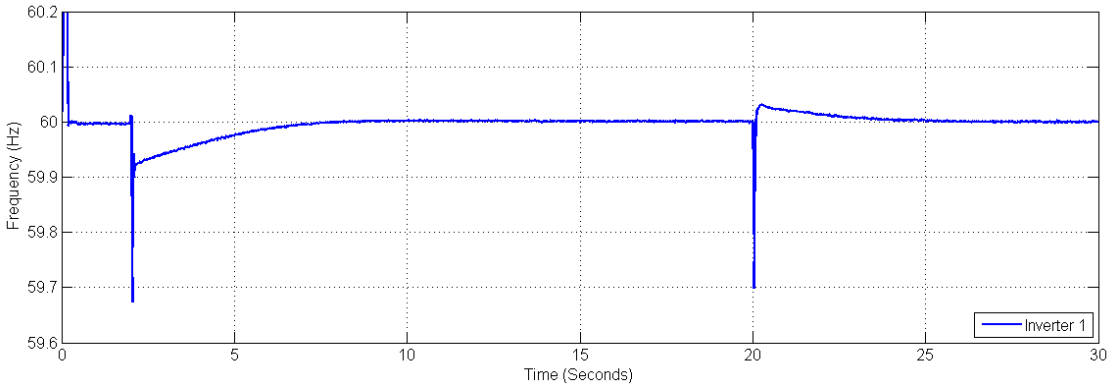

Figure 4-14.: Frequency of the system different layers

Table 4-2.: Microgrid Parameters for non-Identical Agents

Maximum Active Power at each Inverter	$P_{max,1} = 20kW$ $P_{max,2} = 24kW$ $P_{max,3} = 28kW$ $P_{max,4} = 30kW$
Transmission Line Impedances	$Z_{12} = 0{,}23\Omega + j0{,}12$ $Z_{23} = 0{,}35\Omega + j0{,}15$ $Z_{34} = 0{,}5\Omega + j0{,}17$
Load 1 and Load 2	$Load\,1 : 10kW + 3k\text{Var}$ $Load\,2 : 15kW + 5k\text{Var}$
Filter Frequency of Cut (Hz)	$f_1 = 10$ $f_2 = 8$ $f_3 = 4$ $f_4 = 1$
Bus Voltage	V=$120Vrms$
Proportional Gain	$\alpha = 0{,}2$
Integral Gain	$\beta = 0{,}4$

The inverters achieve power sharing when the loads are connected. The effect of different frequencies of cut is more clear for inverter four that has a larger time constant. Different time scales implies a slower response of the system, as Figure **4-15** shows, power sharing is defined by the slower inverter time constant. This effect can be seen also in Figure **4-16**, and Figure **4-17**, where the consensus for proportional and integral layers are shown. Frequency deviations are small enough and the system returns to its nominal value as it is shown in Figure **4-18**. Besides the oscillatory behavior, the frequency of the system is kept within a desirable range, reaching the frequency of reference as it is shown in Figure **4-18**.

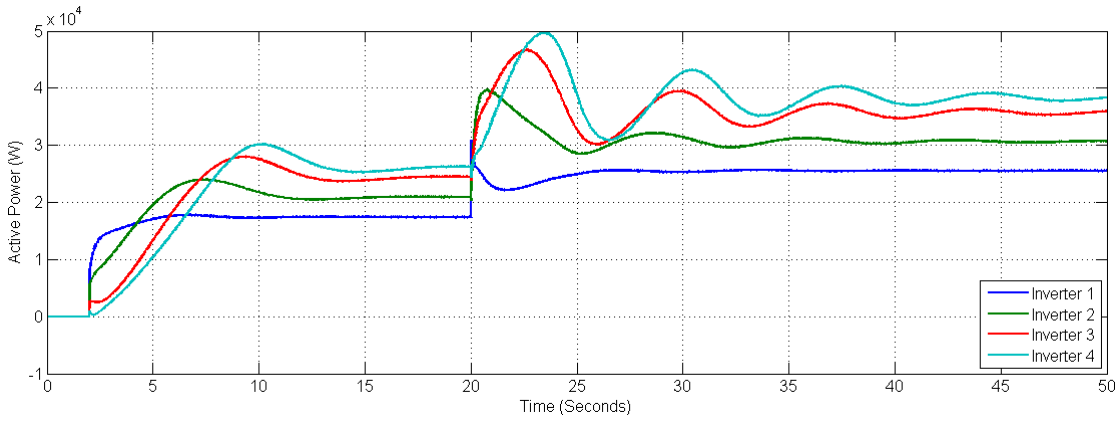

Figure 4-15.: Active power sharing among inverters non-identical agents

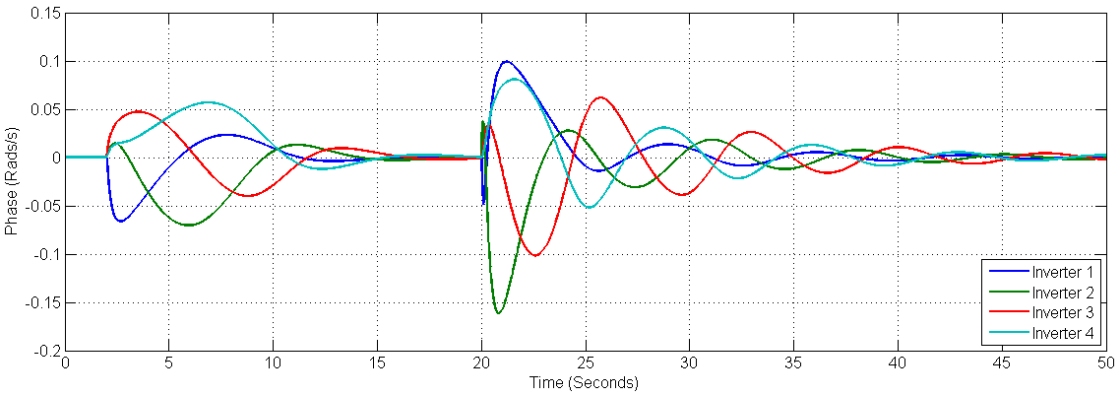

Figure 4-16.: Phase consensus proportional layer non-identical agents

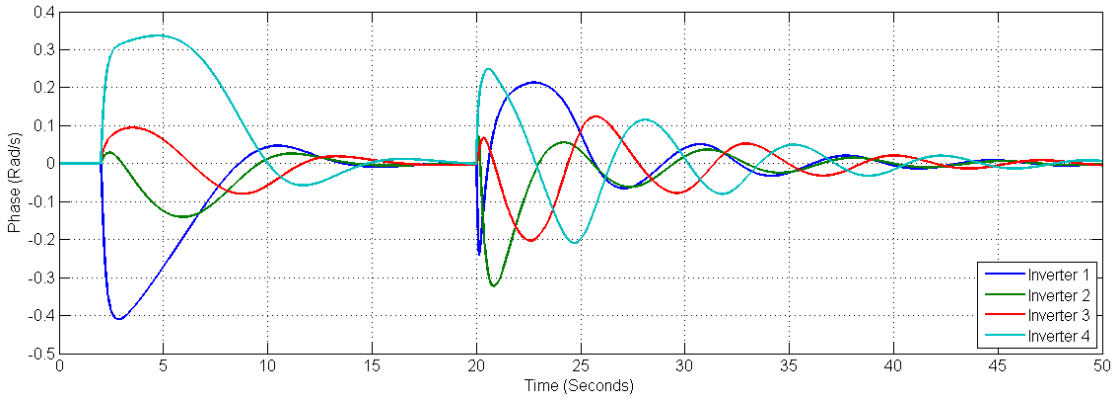

Figure 4-17.: Phase consensus integral layer non-identical agents

4.2. Droop-Free Control for Networked Microgrids

Several microgrids connected through transmission lines form a cluster, those microgrids share information and measurements allowing to generate control signals. Power sharing

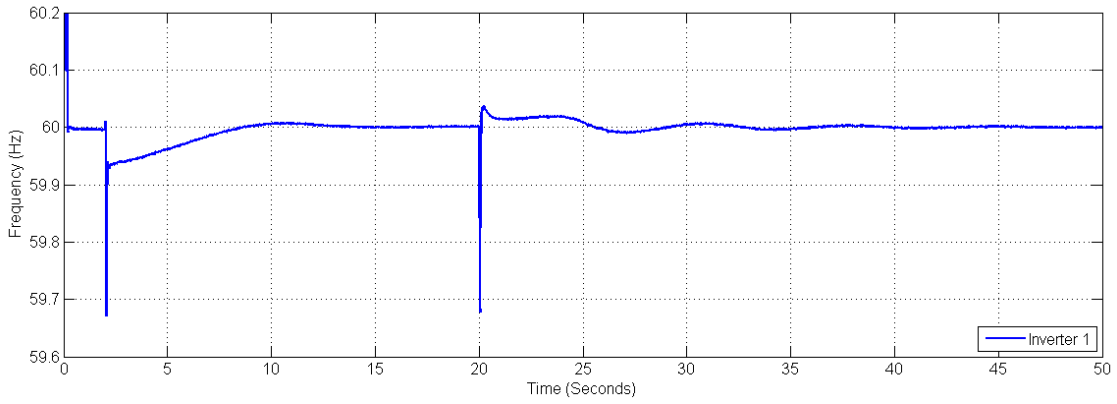

Figure 4-18.: Frequency response for the system with non-identical agents

among microgrids and inverters is a condition desirable. The droop-free paradigm can be implemented in a global form for the networked microgrids.
Inverters inside each microgrid are controlled by (3-17), while microgrids are controlled by a droop-free strategy. Figure **4-19** shows the physical connection among the microgrids for this case in a radial form. Each microgrid is connected to the others through a transformer using the Point of Common Connection (PCC) as it was shown in chapter 3.

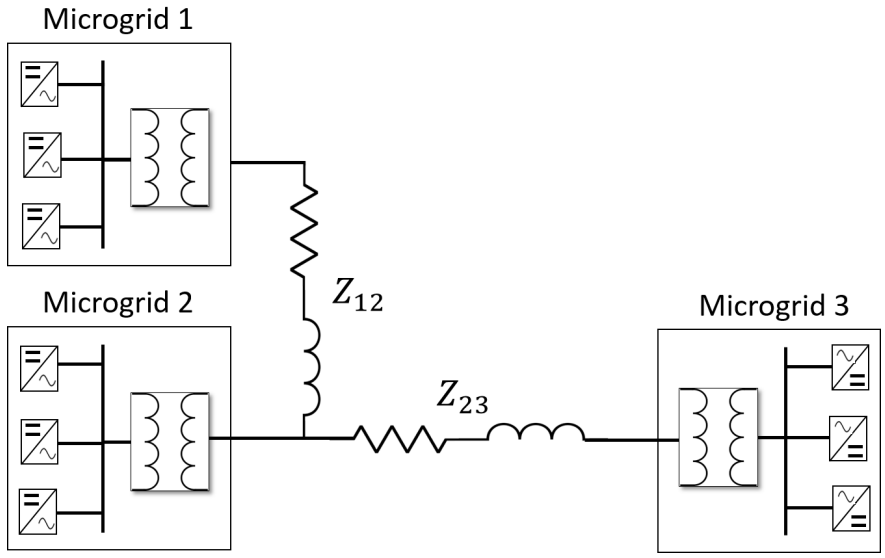

Figure 4-19.: Microgrid physical connection

The matrices for the inverter graph are the same of the system presented before, proportional layer with the case 1 topology, and integral layer with the case 2 topology. Figure **4-20** shows the communication graph among the microgrids inside the cluster, the matrix representation is presented below

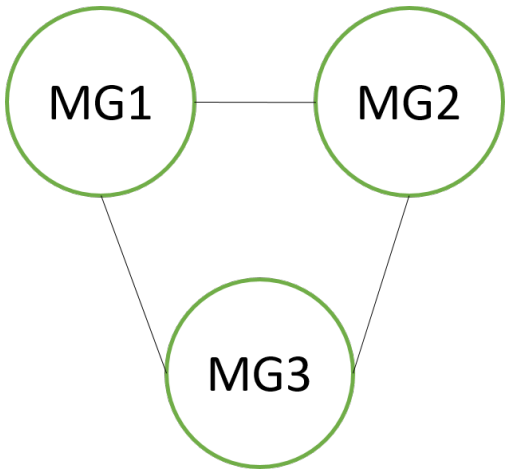

Figure 4-20.: Graph representation for the cluster of microgrids

$$d_{global} = \begin{pmatrix} 2 & 0 & 0 \\ 0 & 2 & 0 \\ 0 & 0 & 2 \end{pmatrix} \qquad A_{global} = \begin{pmatrix} 0 & 1 & 1 \\ 1 & 0 & 1 \\ 1 & 1 & 0 \end{pmatrix} \qquad L_{global} = \begin{pmatrix} 2 & -1 & -1 \\ -1 & 2 & -1 \\ -1 & -1 & 2 \end{pmatrix}$$

Table 4-3.: Microgrid 1 Parameters

Parameter	**Inverter 1**	**Inverter 2**	**Inverter 3**	**Inverter 4**
Inverter Maximum Active Power (kW)	15	18	20	24
Transmission Line Impedances	$Z_{12} = 0{,}23\Omega + j0{,}12 \quad Z_{23} = 0{,}35\Omega + j0{,}15,$ $Z_{34} = 0{,}5\Omega + j0{,}17$			
Load at each Microgrid	$Load_1 = 10$kW+3kVar at $t = 2s$ $Load_2 = 15$kW+5kVar at $t = 30s$			
Filter Frequency of Cut (Hz)	$f_1 = 4$	$f_2 = 4$	$f_3 = 4$	$f_4 = 4$
Proportional Constant Gain	$\alpha = 0{,}2$	$\alpha = 0{,}2$	$\alpha = 0{,}2$	$\alpha = 0{,}2$
Integral Constant Gain	$\beta = 0{,}3$	$\beta = 0{,}3$	$\beta = 0{,}3$	$\beta = 0{,}3$

Table **4-3**, **4-4**, **4-5** and **4-6** show the general parameters for the inverters inside each microgrid, and the microgrids of the cluster, respectively. As in the microgrid case, two loads of are connected, one of $10kW + 3kVA$ at $t = 2s$, and another of $15kW + 5kVA$ at $t = 30s$. Power sharing among microgrids is shown in Figure **4-21**, this is achieved after several seconds due to the effect of low pass filter and consensus cluster gain c. Initially, the consensus

Table 4-4.: Microgrid 2 Parameters

Parameter	Inverter 1	Inverter 2	Inverter 3	Inverter 4
Inverter Maximum Active Power (kW)	15	20	25	25
Transmission Line Impedances	$Z_{12} = 0{,}23\Omega + j0{,}12 \quad Z_{23} = 0{,}35\Omega + j0{,}15,$ $Z_{34} = 0{,}5\Omega + j0{,}17$			
Load at each Microgrid	$Load_1 = 10$kW+3kVar at $t = 2s$ $Load_2 = 15$kW+5kVar at $t = 30s$			
Filter Frequency of Cut (Hz)	$f_1 = 5$	$f_2 = 5$	$f_3 = 5$	$f_4 = 5$
Proportional Constant Gain	$\alpha = 0{,}3$	$\alpha = 0{,}3$	$\alpha = 0{,}3$	$\alpha = 0{,}3$
Integral Constant Gain	$\beta = 0{,}4$	$\beta = 0{,}4$	$\beta = 0{,}4$	$\beta = 0{,}4$

Table 4-5.: Microgrid 3 Parameters

Parameter	Inverter 1	Inverter 2	Inverter 3	Inverter 4
Inverter Maximum Active Power (kW)	20	20	20	20
Transmission Line Impedances	$Z_{12} = 0{,}23\Omega + j0{,}12 \quad Z_{23} = 0{,}35\Omega + j0{,}15,$ $Z_{34} = 0{,}5\Omega + j0{,}17$			
Load at each Microgrid	$Load_1 = 10$kW+3kVar at $t = 2s$ $Load_2 = 15$kW+5kVar at $t = 30s$			
Filter Frequency of Cut (Hz)	$f_1 = 10$	$f_2 = 10$	$f_3 = 10$	$f_4 = 10$
Proportional Constant Gain	$\alpha = 0{,}4$	$\alpha = 0{,}4$	$\alpha = 0{,}4$	$\alpha = 0{,}4$
Integral Constant Gain	$\beta = 0{,}5$	$\beta = 0{,}5$	$\beta = 0{,}5$	$\beta = 0{,}5$

among microgrids is achieved faster at $t = 2s$ due all active power start at zero. At $t = 30s$, power sharing is achieved in approximately $60s$ due the differences among transmission lines and inverter power ratings.

The consensus among microgrids is shown in Figure **4-22**. First, the consensus is achieved after connecting a load at $t = 2s$. At $t = 30s$ consensus is achieved after almost one minute, notice that the values for the consensus variables are smaller compared with the values for the consensus among inverters.

Table 4-6.: Cluster Parameters

Parameter	Microgrid 1	Microgrid 2	Microgrid 3
Maximum Active Power at each microgrid (kW)	77	85	80
Transmission Line Impedances	$Z_{12} = j0{,}37$ $Z_{23} = j0{,}45$		
Filter Frequency of Cut (Hz)	$f_1 = 0{,}25$	$f_2 = 0{,}25$	$f_1 = 0{,}25$
Consensus Gain	$c = 0{,}15$	$c = 0{,}15$	$c = 0{,}15$

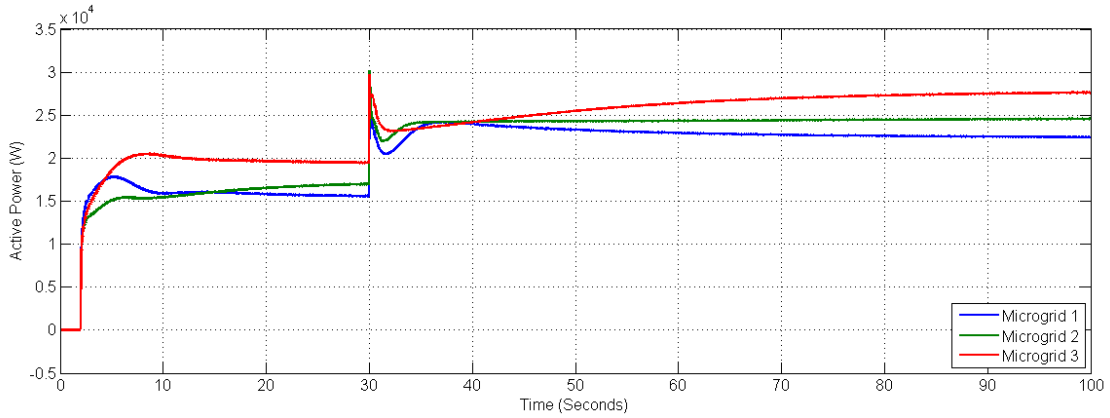

Figure 4-21.: Active power sharing among microgrids

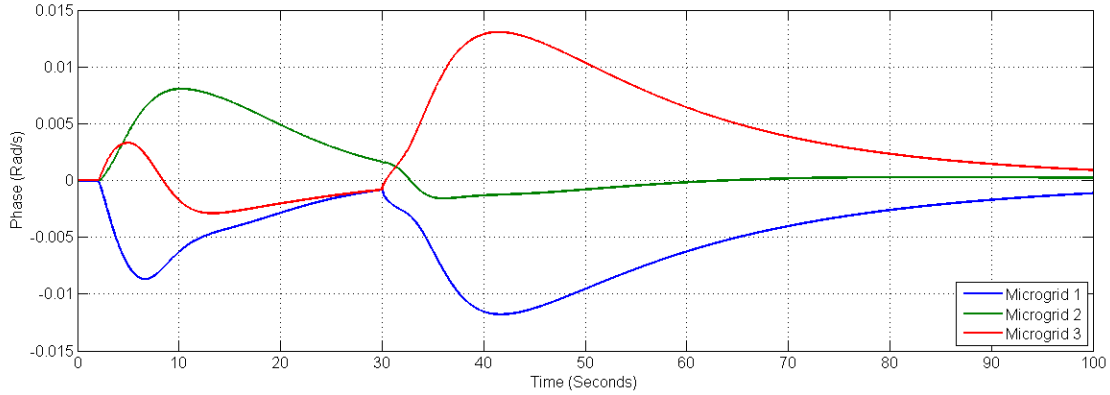

Figure 4-22.: Consensus among microgrids

Power sharing among inverters is not affected by the consensus signal from the microgrids as can be seen in Figure **4-23**. Consensus among inverters is achieved in less time than for microgrids and presents a little oscillation when the second load is connected at $t = 30s$.

The consensus among inverters is achieved in less than $20s$ as it is shown in Figure **4-24** for

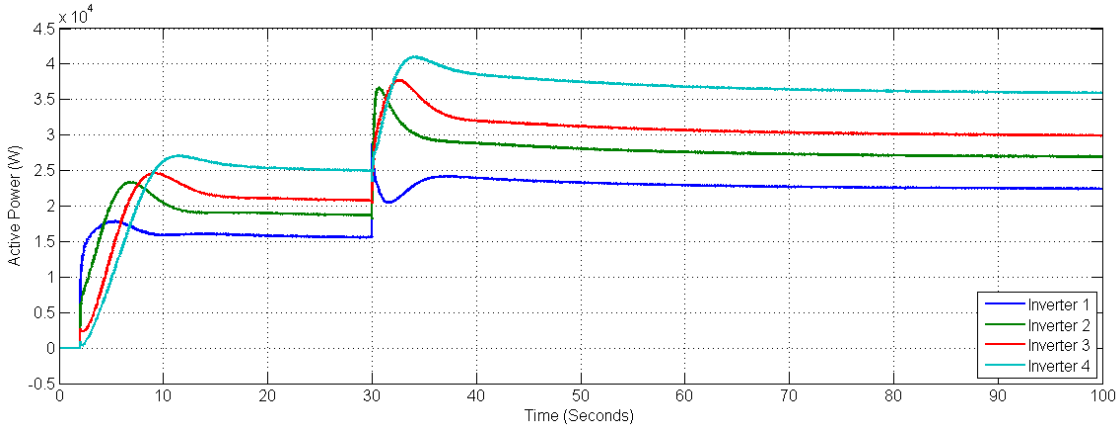

Figure 4-23.: Power sharing among inverters of microgrid 1

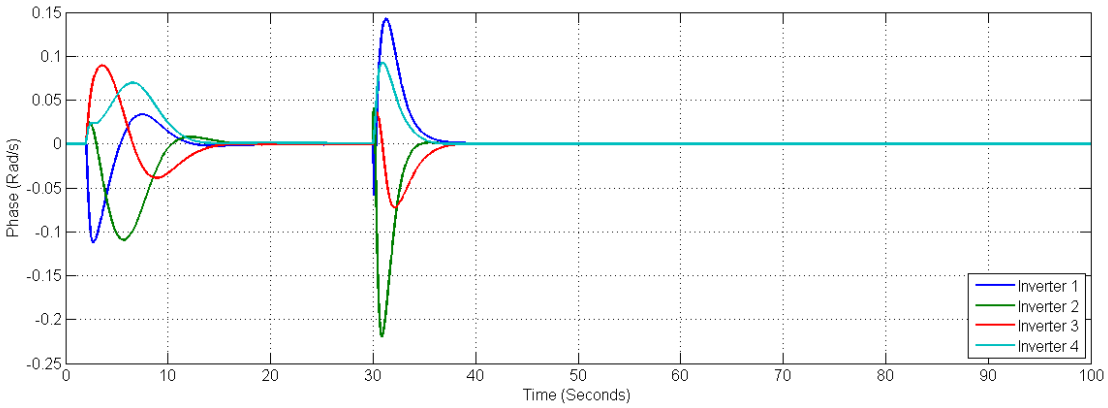

Figure 4-24.: Proportional term among inverters of microgrid 1

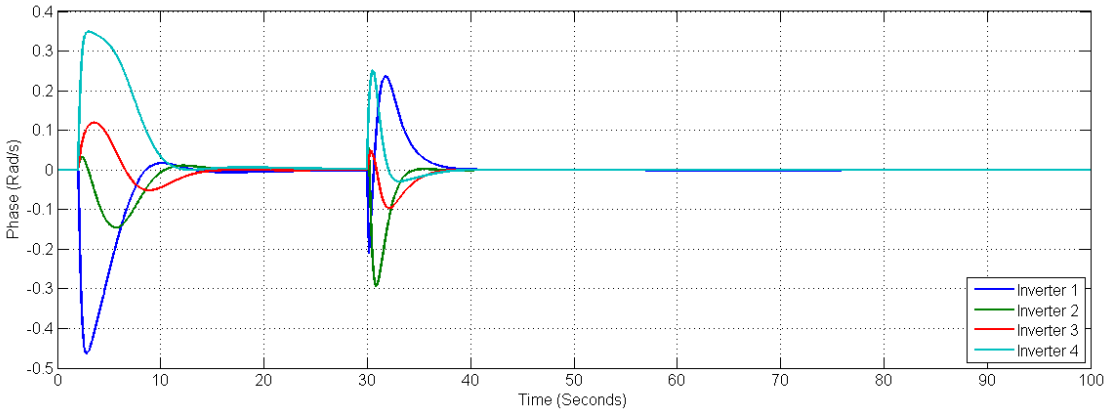

Figure 4-25.: Integral term among inverters of microgrid 1

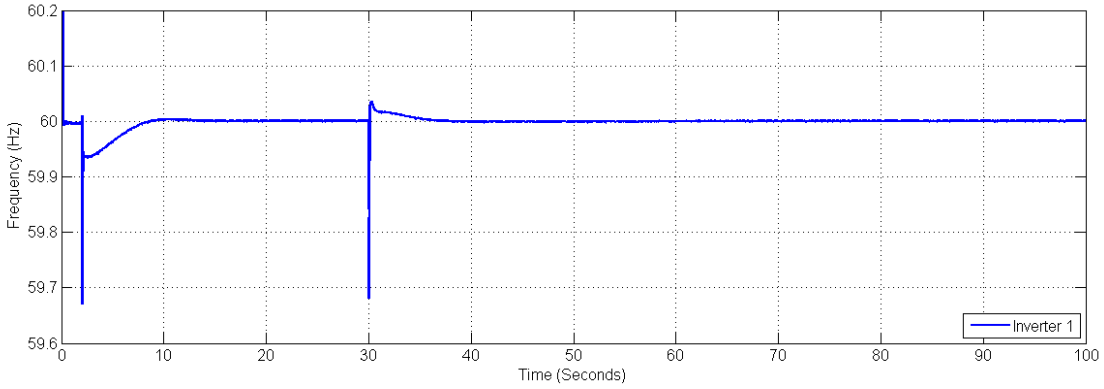

Figure 4-26.: Frequency of the cluster

the proportional layer, and Figure **4-25** for the integral layer. Those values are bigger than the values from microgrid consensus. The frequency of the system is shown in Figure **4-26**. Frequency variations can be seen at $t = 2s$ and $t = 30s$, and are inside the acceptable limits. The connection or release of charges of the system generates frequency oscillations that last for several seconds, this behavior is caused principally by the inverters time response.

4.3. Effects of Some Variables at Consensus

Several variables have a remarkable effect on the achievement of consensus among them are the frequency of cut of low-pass filters, consensus gain for proportional and integral layers, and maximum active power ratings. The effect of different values of those variables is analyzed in this section.

Table 4-7.: Microgrid Parameters All Cases

Parameter	**Inverter 1**	**Inverter 2**	**Inverter 3**	**Inverter 4**
Transmission Line Impedances	$Z_{12} = 0{,}23\Omega + j0{,}12$ $Z_{23} = 0{,}35\Omega + j0{,}15$, $Z_{34} = 0{,}5\Omega + j0{,}17$			
Load at each Microgrid	$Load_1 = 10$kW+3kVar at $t = 2s$ $Load_2 = 15$kW+5kVar at $t = 20s$			

4.3.1. Low-Pass Filter Frequency of Cut

An agent in a distributed system, in this case, an inverter, with a low-pass filter frequency of cut smaller than the other inverters (see Table **4-8**), provoke that the consensus achievement becomes slower than in a case with identical agents, and generates an oscillatory behavior. In any case, consensus is achieved, but the time of the consensus achievement depends on

the time constant of the inverter with the smaller frequency of cut.

Table 4-8.: Microgrid Parameters Frequency of Cut Effect

Parameter	Inverter 1	Inverter 2	Inverter 3	Inverter 4
Maximum Active Power at each inverter (kW)	20	20	20	20
Filter Frequency of Cut (Hz)	$f_1 = 20$	$f_2 = 20$	$f_3 = 1$	$f_4 = 1$
Proportional Constant Gain	$\alpha = 0{,}2$	$\alpha = 0{,}2$	$\alpha = 0{,}2$	$\alpha = 0{,}2$
Integral Constant Gain	$\beta = 0{,}4$	$\beta = 0{,}4$	$\beta = 0{,}4$	$\beta = 0{,}4$

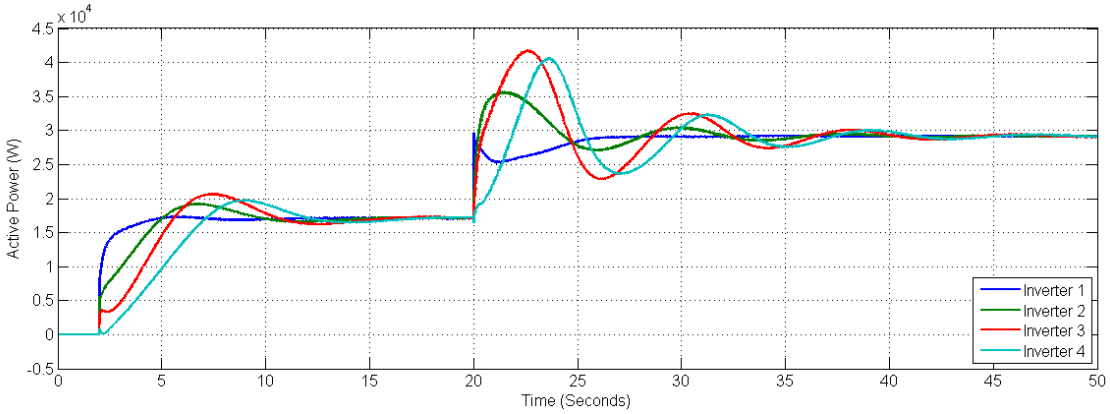

Figure 4-27.: Power sharing among inverters with different filter frequencies

Figure **4-27**, **4-28**, and **4-29** show the behavior for power sharing and proportional and integral layers for consensus among inverters with identical maximum power capacity and different frequencies of cut. The oscillatory behavior decay as time gone. Inverters three and four have the higher oscillations which is in order with the lower frequency of these. Thus, frequencies of cut among agents can not be remarkably different.

4.3.2. Maximum Active Power

Different maximum active power ratings among agents (inverters or microgrid), do not have an important effect on consensus and power sharing achievement. As active power measured is normalized by the maximum power value, consensus responses do not show an oscillatory

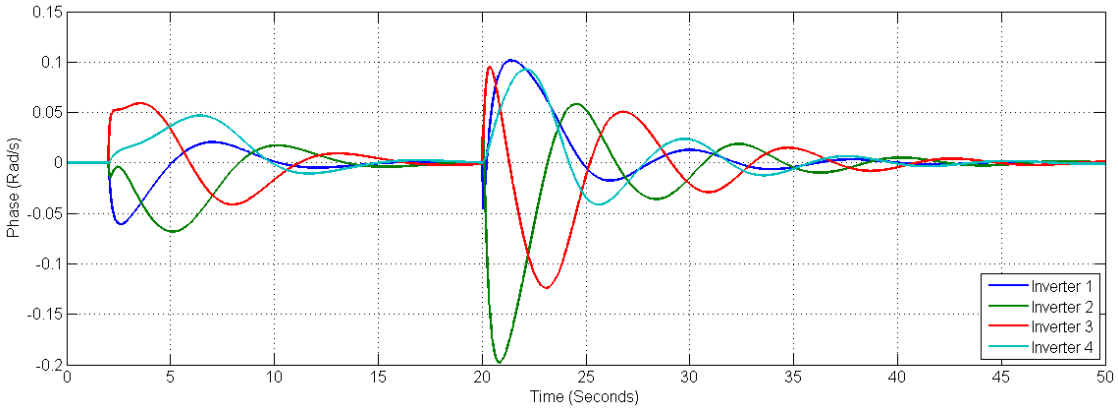

Figure 4-28.: Consensus behavior for inverters with different filter frequencies

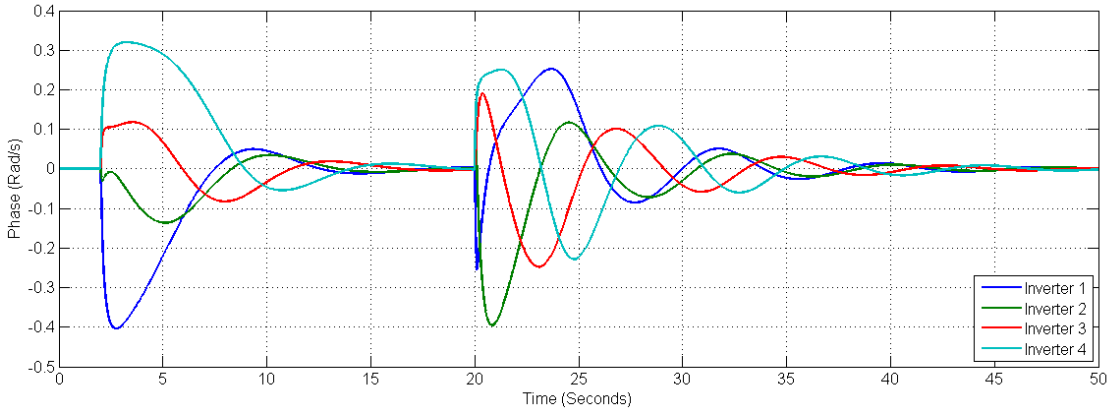

Figure 4-29.: Consensus behavior for inverters with different filter frequencies

behavior.

Table **4-9**, resumes the parameters for the inverters of a microgrid, at this case, two inverters have a higher power rating than the two others. The frequency of cut parameter is the same for each one. At Figure **4-30**, inverters one and two supply more active power than inverters three and four. It is notable that there is not an oscillatory behavior as inverters assume a bigger quantity of power, the proportional and integral layers achieves consensus rapidly as is shown in Figure **4-31** and Figure **4-32**.

4.3.3. Different Consensus Gains

Each agent of a multi-agent system can set the gain of its own consensus equation. This value, as was presented before, determines the velocity of the consensus. This velocity is limited by the energy of the system and maximum peak allow by the physical system.

Table 4-9.: Microgrid Parameters Different Maximum Active Power Ratings

Parameter	Inverter 1	Inverter 2	Inverter 3	Inverter 4
Maximum Active Power at each inverter (kW)	30	30	10	10
Filter Frequency of Cut (Hz)	$f_1 = 5$	$f_2 = 5$	$f_3 = 5$	$f_4 = 5$
Proportional Constant Gain	$\alpha = 0{,}2$	$\alpha = 0{,}2$	$\alpha = 0{,}2$	$\alpha = 0{,}2$
Integral Constant Gain	$\beta = 0{,}4$	$\beta = 0{,}4$	$\beta = 0{,}4$	$\beta = 0{,}4$

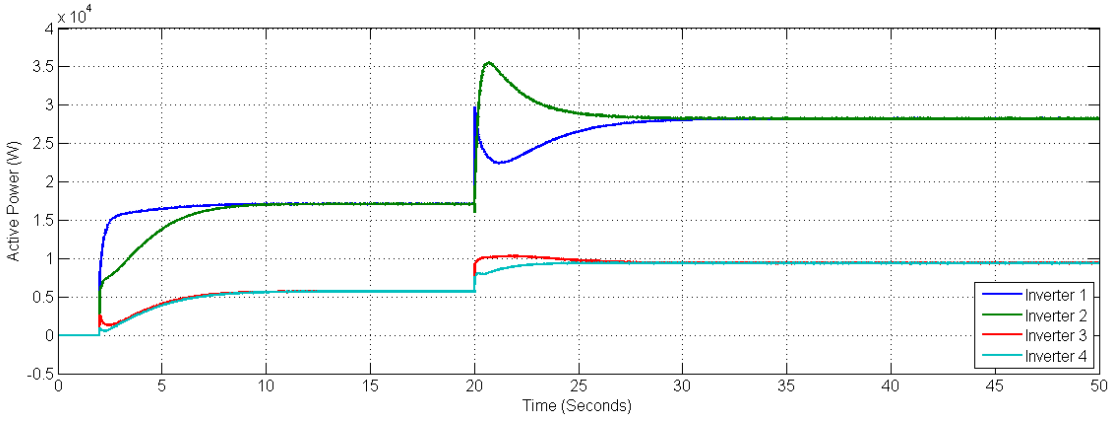

Figure 4-30.: Power sharing effect of one inverter with different maximum active power

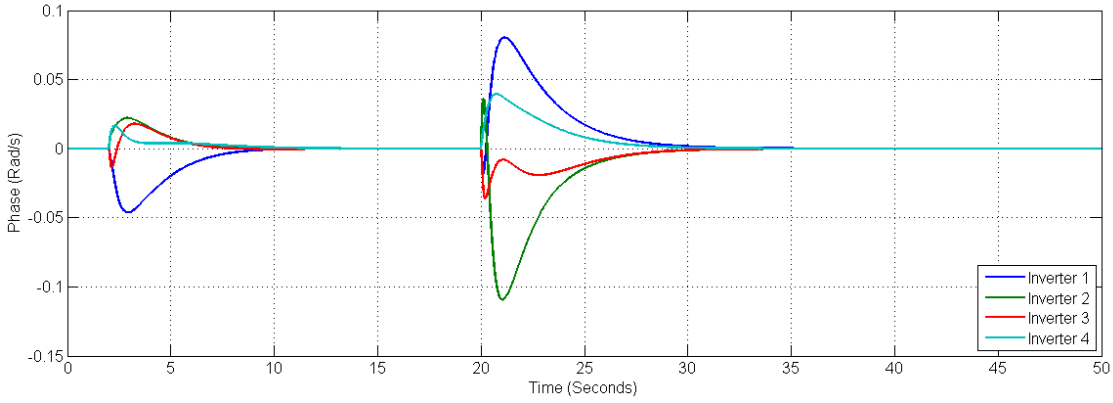

Figure 4-31.: Consensus effect of one inverter with different maximum active power

Four inverters with identical maximum active power and frequencies of cut are simulated with different consensus gain constant for the proportional and integral layers at each inverter

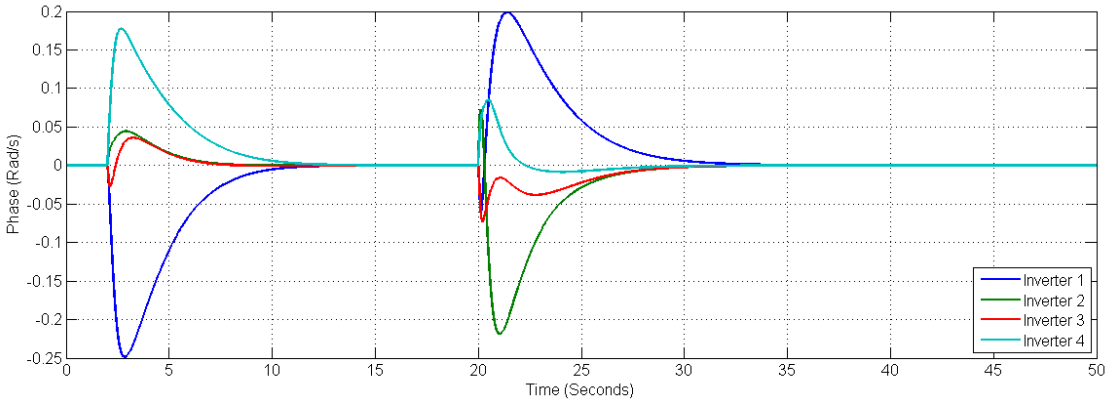

Figure 4-32.: Consensus effect of one inverter with different maximum active power

Table 4-10.: Microgrid Parameters Different Consensus Gains for the Agents

Parameter	Inverter 1	Inverter 2	Inverter 3	Inverter 4
Maximum Active Power at each inverter (kW)	20	20	20	20
Filter Frequency of Cut (Hz)	$f_1 = 4$	$f_2 = 4$	$f_3 = 4$	$f_4 = 4$
Proportional Constant Gain	$\alpha = 0{,}05$	$\alpha = 0{,}1$	$\alpha = 0{,}2$	$\alpha = 0{,}5$
Integral Constant Gain	$\beta = 0{,}05$	$\beta = 0{,}1$	$\beta = 0{,}2$	$\beta = 0{,}5$

(see Table **4-10**).

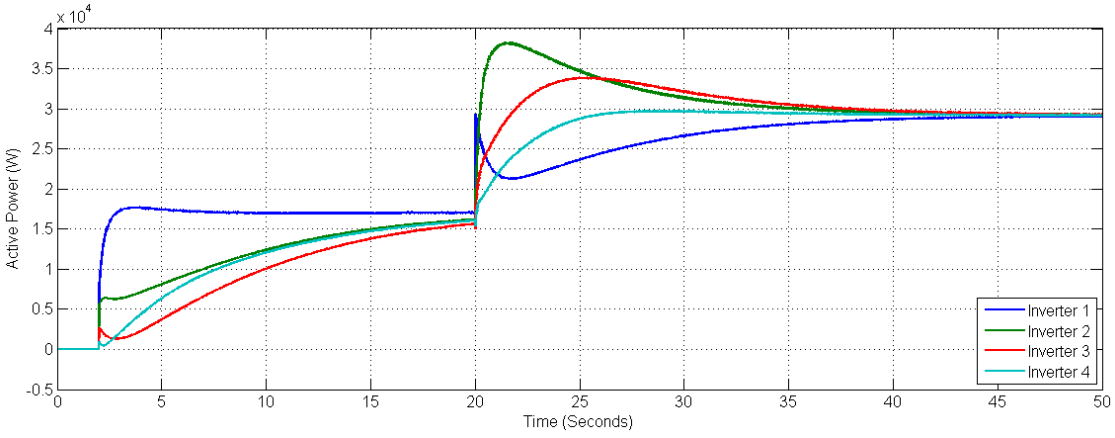

Figure 4-33.: Power sharing among inverters with different consensus gains

The effect of different consensus gains in power sharing can be seen in Figure **4-33**, in this case, the system response and the low-pass filter limit the change of the active power. The global consensus achievement is not determined by the local consensus gain but implies that the agents with the smaller consensus gain have to generate higher values at control correction terms in order to reach the values of the agents with bigger consensus gains. This action can be seen clearly at Figure **4-34** and Figure **4-35**.

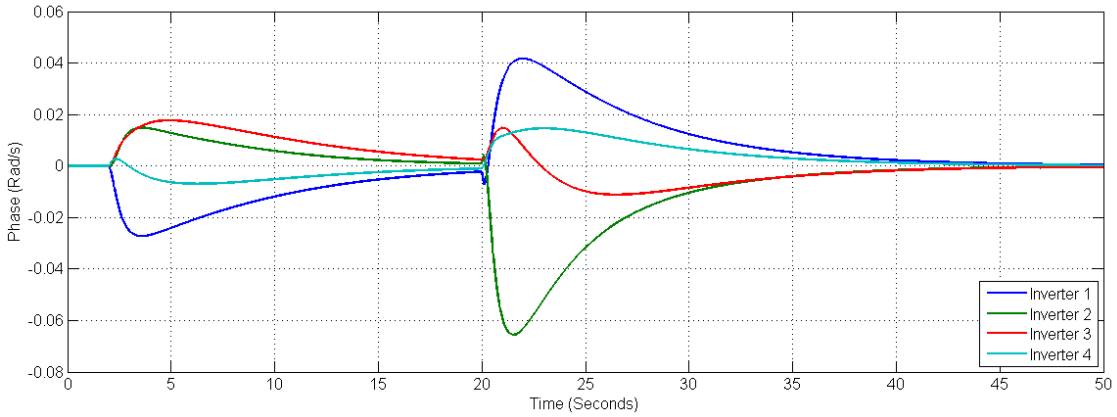

Figure 4-34.: Consensus behavior for different gains

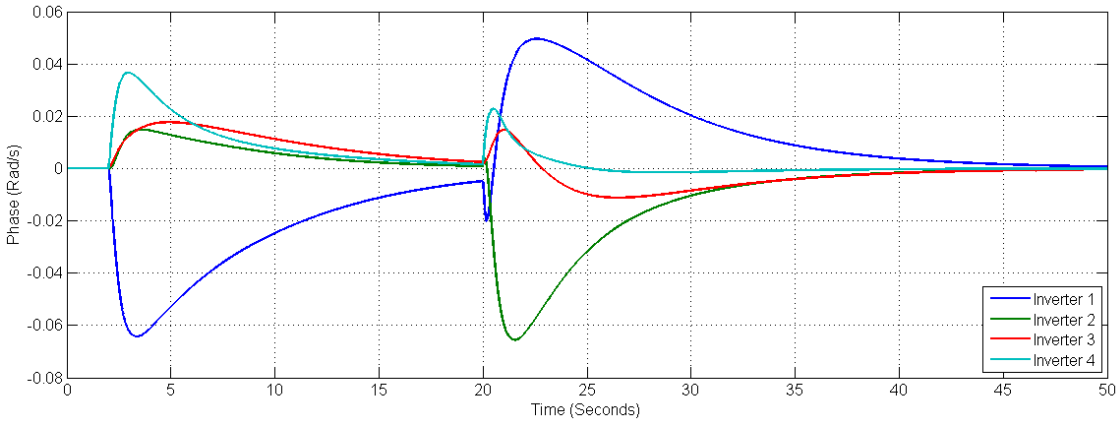

Figure 4-35.: Consensus behavior for different gains

5. Conclusions and Recommendations

5.1. Conclusions

Tertiary control for a cluster can be design to achieve power sharing among microgrids, based on the same principle of droop-free secondary control. In both cases, active and reactive power are assumed decoupled and controlled by frequency and voltage, respectively.

Microgrid and cluster design are based on a set of simple equations that allows making several simplifications, getting a general design in which the model does not affect the controller performance enhancing the scalability and plug and play capacity of the system.

The proposed controller allows controlling a microgrid cluster and the inverters inside each microgrid in a distributed way. Several variables that make the agents non-identical are considered. Based on the distributed PI action from the selected bibliography, the control signals are generated for a set of heterogeneous agents without the necessity of developing an exosystem or an elaborate model of the agents.

The principal aspects that make the agent non-identical are the impedance value among inverters and microgrids, low-pass filter time constant, and proportional and integral distributed values. Changes in this values does not affect the stability of the system, in fact, poles move away along the real axis to the left part of the complex plane.

Frequency control is based on the relationship between phase and frequency, in fact, the droop-free control and phase-droop control act directly over the phase term at each inverter. The condition for those controllers is given by the expression $\theta < \frac{\pi}{2}$; thus the consensus gain for the distributed controller can not be too large. The global controller does not affect the stability of the system because the global term is always very much little than the local term.

The performance of a control system based on homogeneous agent theory is not so different from a control based on heterogeneous agents. The aspects that make the agents non-identical do not have a considerable effect on the dynamic of a system. In fact, low-pass filter constants are the features that have a major effect on consensus achievement generating an oscillatory behavior before steady state is reached.

5.2. Recommendations

Control of a cluster of microgrids is a field that can be studied not only from the islanded perspective but since the interaction of the microgrids with the utility network too. The analysis of the system will be made considering the effects of the network on the behavior of the microgrid, and the way in which is defined the cluster.

The interconnection of several microgrids needs not only to guarantee the power sharing condition but an energy management system, which can control the power flow based on economic and technical decision to optimize the consumption and generation of energy.

It is important to include the voltage control in the control design to guarantee a better performance of the whole system from the inverter and microgrid perspective. This voltage control will be capable of improving the voltage regulation and, in the same time, the reactive power sharing. This item implies a more sophisticated control in the case of a cluster of microgrids based on the fact that voltage is not a global variable as frequency.

Future works must include aspects of power quality related with distributed generator and storage systems because a more detailed analysis of the voltage and frequency disturbances generated by the control action is not one of the objectives of this work.

Time-scale separation is presented as an alternative to managing several control layers in a hierarchical model. However, it is important to establish better-elaborated criteria to decided the limits in which the action of the controller can affect the behavior of the other layer.

It is important the development of experiments of interconnected microgrids, to analyze the behavior of the proposed controllers in hardware. Even when other authors have done some experiments, the interconnection of several islanded AC microgrids have been not presented yet.

A. Appendix: Simulink Simulation Model

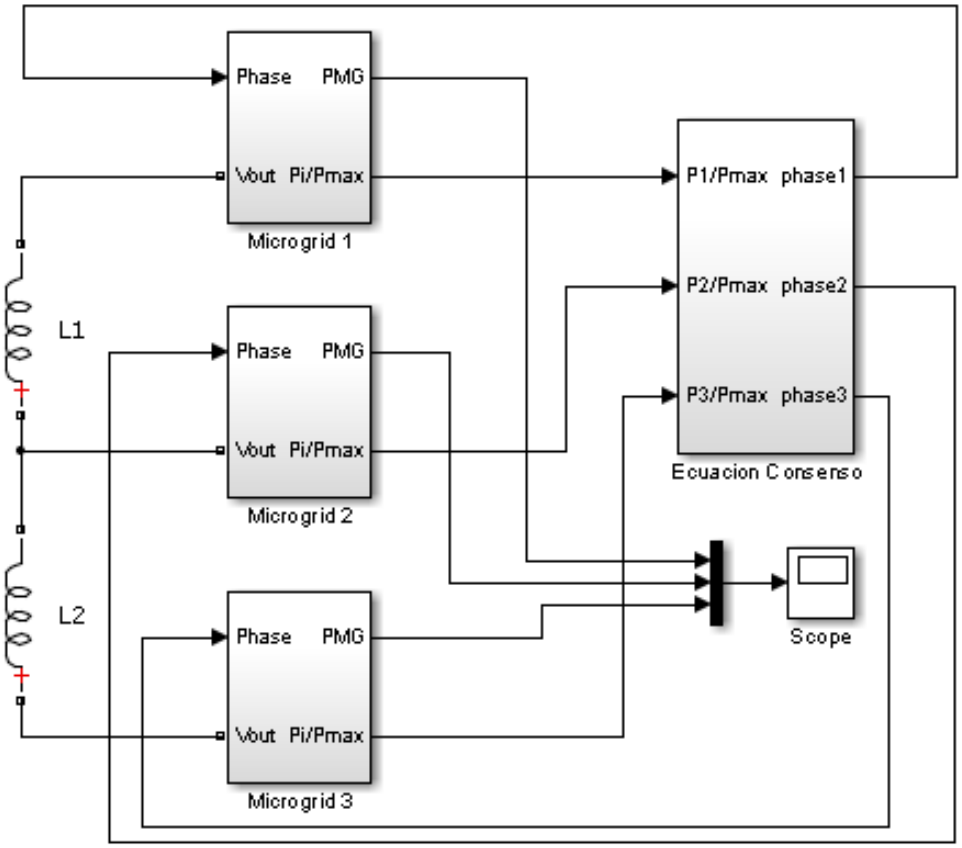

Figure A-1.: Simulink cluster diagram

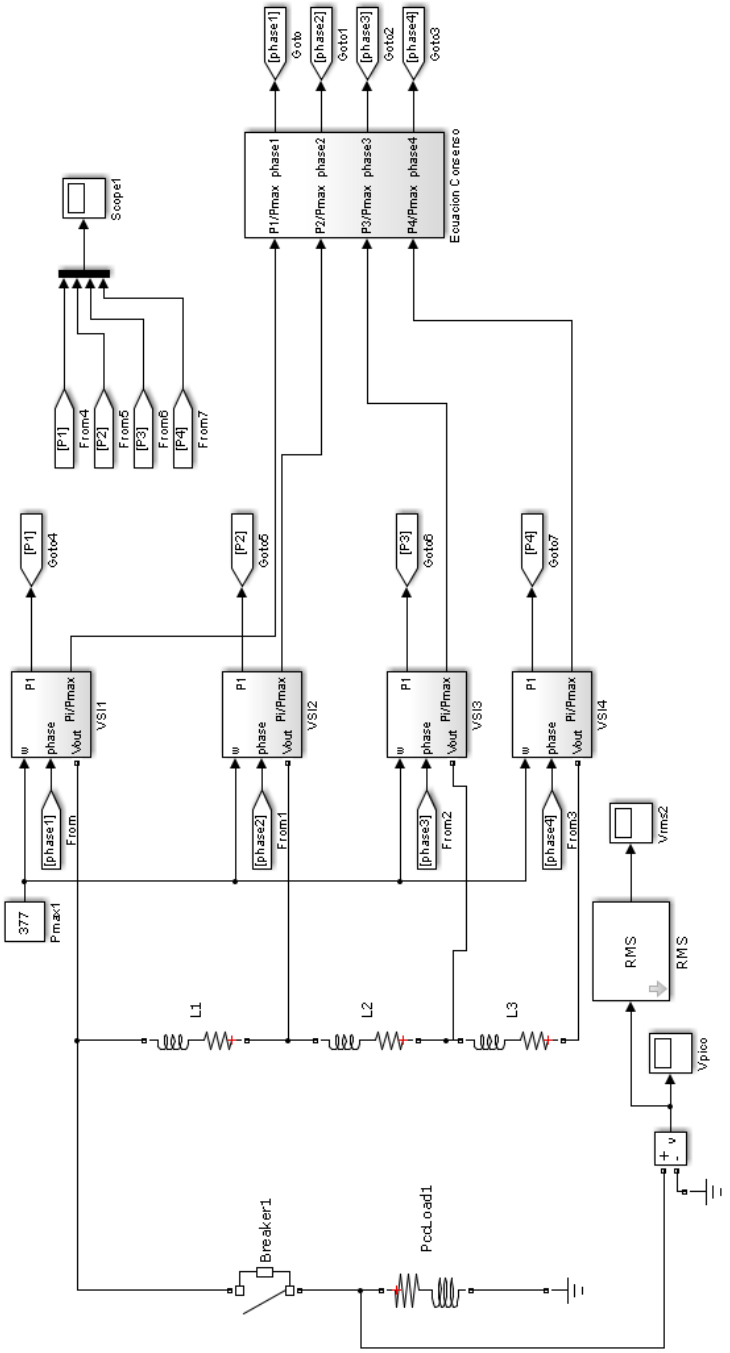

Figure A-2.: Inverter connection inside a microgrid

A.0.1. Matlab Code

```
function [sys,x0,str,ts] = ConsensoInversor(t,x,u,flag)
switch flag,
case 0
[sys,x0,str,ts] = mdlInitializeSizes;
case 3
sys = mdlOutputs(t,x,u);
case  1, 2, 4, 9
sys = [];
otherwise
error(['Unhandled flag = ',num2str(flag)]);
end;
function [sys,x0,str,ts] = mdlInitializeSizes
sizes = simsizes;
sizes.NumContStates= 0;
sizes.NumDiscStates= 0;
sizes.NumOutputs= 4;
sizes.NumInputs= 4;
sizes.DirFeedthrough=1;
sizes.NumSampleTimes=1;
sys = simsizes(sizes);
x0 = [];
str = [];
ts = [0 0];
function sys = mdlOutputs(t,x,u)
Case 1
A=[0 1 0 0; 1 0 1 0; 0 1 0 1; 0 0 1 0];
Case 2
A=[0 1 1 1; 1 0 1 1;1 1 0 1; 1 1 1 0];
Case 3
A=[0 1 0 0; 1 0 1 1;0 1 0 1; 0 1 1 0];
N=4;
DX=zeros(4,1);
for i=1:N;
for j=1:N;
if (A(i,j)==1);
DX(i,:)=DX(i,:)+1.0*((u(j,:)-u(i,:)));
end
end
```

```
end
sys=0.3*DX;
End of mdlOutputs.
```

Bibliografía

[1] N. Hatziargyriou, H. Asano, R. Iravani, and C. Marnay, "Microgrids," *IEEE Power and Energy Magazine*, vol. 5, no. 4, pp. 78–94, 2007.

[2] R. H. Lasseter, "MicroGrids," *IEEE Power Engineering Society winter Meeting*, pp. 305–308, 2002.

[3] F. Katiraei, R. Iravani, N. Hatziargyriou, and A. Dimeas, "Microgrids management," *IEEE Power and Energy Magazine*, vol. 6, no. 3, pp. 54–65, 2008.

[4] P. C. Loh, S. Member, D. Li, Y. K. Chai, and F. Blaabjerg, "Autonomous Operation of Hybrid Microgrid With AC and DC Subgrids," vol. 28, no. 5, pp. 2214–2223, 2013.

[5] A. F. Moreno and E. Mojica-Nava, "Lvdc microgrid perspective for a high efficiency distribution system," in *Transmission & Distribution Conference and Exposition-Latin America (PES T&D-LA), 2014 IEEE PES*, pp. 1–7, IEEE, 2014.

[6] J. Lopes, C. Moreira, and A. Madureira, "Defining Control Strategies for MicroGrids Islanded Operation," *IEEE Transactions on Power Systems*, vol. 21, no. 2, pp. 916–924, 2006.

[7] J. M. Guerrero, J. C. Vásquez, and R. Teodorescu, "Hierarchical control of droop-controlled DC and AC microgrids - A general approach towards standardization," *IECON Proceedings (Industrial Electronics Conference)*, pp. 4305–4310, 2009.

[8] A. Bidram, F. L. Lewis, A. Davoudi, and Z. Qu, "Frequency control of electric power microgrids using distributed cooperative control of multi-agent systems," *2013 IEEE International Conference on Cyber Technology in Automation, Control and Intelligent Systems*, pp. 223–228, 2013.

[9] F. L. Lewis, Z. Qu, A. Davoudi, and A. Bidram, "Secondary control of microgrids based on distributed cooperative control of multi-agent systems," *IET Generation, Transmission & Distribution*, vol. 7, no. October 2012, pp. 822–831, 2013.

[10] Y. Zheng, L. Wang, and Y. Zhu, "Consensus of heterogeneous multi-agent systems," *IET Control Theory & Applications*, vol. 5, no. 16, pp. 1881–1888, 2011.

[11] J. Shao, J. Wang, and T. Yang, "Experimental validation of distributed cooperative control for mobile agents with switching topologies and time-delays," *IEEE International Conference on Electro/Information Technology*, vol. 0, pp. 512–517, 2014.

[12] J. Zhao, D. J. Hill, and T. Liu, "Passivity-based output synchronization of dynamical networks with non-identical nodes," *Proceedings of the IEEE Conference on Decision and Control*, no. 3, pp. 7351–7356, 2010.

[13] J. J. Justo, F. Mwasilu, J. Lee, and J. W. Jung, "AC-microgrids versus DC-microgrids with distributed energy resources: A review," *Renewable and Sustainable Energy Reviews*, vol. 24, pp. 387–405, 2013.

[14] H. Farhangi, "The path of the smart grid," *IEEE Power and Energy Magazine*, vol. 8, no. 1, pp. 18–28, 2010.

[15] X. Fang, S. Misra, G. Xue, and D. Yang, "Smart Grid — The New and Improved Power Grid: A Survey," *IEEE Communications Surveys & Tutorials*, vol. 14, no. 4, pp. 944–980, 2012.

[16] A. Tuladhar, H. Jin, T. Unger, and K. Mauch, "Parallel operation of single phase inverter modules with no control interconnections," *Proceedings of APEC 97 - Applied Power Electronics Conference*, vol. 1, pp. 94–100, 1997.

[17] J. M. Guerrero, L. G. de Vicuna, J. Matas, M. Castilla, and J. Miret, "A wireless controller to enhance dynamic performance of parallel inverters in distributed generation systems," *IEEE Transactions on Power Electronics*, vol. 19, no. 5, pp. 1205–1213, 2004.

[18] E. Coelho, P. Cortizo, and P. Garcia, "Small signal stability for single phase inverter connected to stiff\nAC system," *Conference Record of the 1999 IEEE Industry Applications Conference. Thirty-Forth IAS Annual Meeting (Cat. No.99CH36370)*, vol. 4, pp. 2180–2187, 1999.

[19] J. Rocabert, A. Luna, F. Blaabjerg, and I. Paper, "Control of Power Converters in AC Microgrids.pdf," *IEEE Transactions on Power Electronics*, vol. 27, no. 11, pp. 4734–4749, 2012.

[20] A. Bidram and A. Davoudi, "Hierarchical structure of microgrids control system," *IEEE Transactions on Smart Grid*, vol. 3, no. 4, pp. 1963–1976, 2012.

[21] G.-i. Scheme, M. Castilla, L. Garc, J. Miret, and J. C. Vasquez, "Virtual Impedance Loop for Droop-Controlled Single-Phase Parallel Inverters Using a Second-Order," vol. 25, no. 12, pp. 2993–3002, 2010.

[22] M. Farrokhabadi and C. A. Ca, "Evaluation of Droop-Based Controls in an Islanded Microgrid with Electronically Interfaced Distributed Energy Resources,"

[23] R. Majumder and A. Ghosh, "Operation and Control of Hybrid Microgrid with Angle Droop Controller," no. 1, pp. 509–515, 2010.

[24] H. Moussa, S. Member, A. Shahin, S. Member, F. Sharif, J.-p. Martin, S. Pierfederici, and V. L. Nancy, "Optimal Angle Droop Power Sharing Control for Autonomous Microgrid," pp. 506–511, 2015.

[25] R. Majumder, S. Member, and A. Ghosh, "Angle Droop versus Frequency Droop in a Voltage Source Converter Based Autonomous Microgrid," 2009.

[26] M. Andreasson, D. V. Dimarogonas, H. Sandberg, and K. H. Johansson, "Distributed PI-control with applications to power systems frequency control," *2014 American Control Conference*, pp. 3183–3188, 2014.

[27] Q. Shafiee, J. C. Vasquez, J. M. Guerrero, V. Nasirian, and A. Davoudi, "Cooperative frequency control for autonomous AC Microgrids," *2015 IEEE Eindhoven PowerTech, PowerTech 2015*, 2015.

[28] Q. Shafiee, J. M. Guerrero, and J. C. Vasquez, "Distributed secondary control for islanded microgrids-a novel approach," *IEEE Transactions on Power Electronics*, vol. 29, no. 2, pp. 1018–1031, 2014.

[29] V. Nasirian, Q. Shafiee, J. M. Guerrero, F. L. Lewis, and A. Davoudi, "Droop-Free Distributed Control for AC Microgrids," *IEEE Transactions on Power Electronics*, vol. 31, no. 2, pp. 1600–1617, 2016.

[30] J. M. Guerrero, J. C. Vásquez, M. Savaghebi, J. D. Hoz, and H. Martín, "Hierarchical Control of Power Plants with Microgrid Operation," *Annual Conference on IEEE Industrial Electronics Society*, pp. 3006–3011, 2010.

[31] C. M. Shepherd, "Design of primary and secondary cells ii. an equation describing battery discharge," *Journal of the Electrochemical Society*, vol. 112, no. 7, pp. 657–664, 1965.

[32] L. H. Saw, K. Somasundaram, Y. Ye, and A. A. O. Tay, "Electro-thermal analysis of Lithium Iron Phosphate battery for electric vehicles," *Journal of Power Sources*, vol. 249, pp. 231–238, 2014.

[33] O. Tremblay and L. A. Dessaint, "Experimental validation of a battery dynamic model for EV applications," *World Electric Vehicle Journal*, vol. 3, no. 1, pp. 289–298, 2009.

[34] M. Mesbahi and M. Egerstedt, *Graph theoretic methods in multiagent networks*. Princeton University Press, 2010.

[35] R. Olfati-Saber, J. A. Fax, and R. M. Murray, "Consensus and cooperation in networked multi-agent systems," *Proceedings of the IEEE*, vol. 95, no. 1, pp. 215–233, 2007.

[36] Y.-P. Tian, *Frequency-domain analysis and design of distributed control systems*. John Wiley & Sons, 2012.

[37] H. Zhang, F. L. Lewis, and Z. Qu, "Lyapunov, adaptive, and optimal design techniques for cooperative systems on directed communication graphs," *IEEE Transactions on Industrial Electronics*, vol. 59, no. 7, pp. 3026–3041, 2012.

[38] H. K. Khalil and J. Grizzle, *Nonlinear systems*, vol. 3. Prentice hall New Jersey, 1996.

[39] T. Yang, A. Saberi, A. A. Stoorvogel, and H. F. Grip, "Output synchronization for heterogeneous networks of introspective right-invertible agents," *International journal of robust and nonlinear control*, vol. 24, no. 13, pp. 1821–1844, 2014.

[40] H. F. Grip, T. Yang, A. Saberi, and A. A. Stoorvogel, "Output synchronization for heterogeneous networks of non-introspective agents," *Automatica*, vol. 48, no. 10, pp. 2444–2453, 2012.

[41] P. Wieland, R. Sepulchre, and F. Allg??wer, "An internal model principle is necessary and sufficient for linear output synchronization," *Automatica*, vol. 47, no. 5, pp. 1068–1074, 2011.

[42] H. Kim, H. Shim, and J. H. Seo, "Output consensus of heterogeneous uncertain linear multi-agent systems," *IEEE Transactions on Automatic Control*, vol. 56, no. 1, pp. 200–206, 2011.

[43] R. Carli, E. D'Elia, and S. Zampieri, "A PI controller based on asymmetric gossip communications for clocks synchronization in wireless sensors networks," *Proceedings of the IEEE Conference on Decision and Control*, pp. 7512–7517, 2011.

[44] G. S. Seyboth and F. Allgöwer, "Output synchronization of linear multi-agent systems under constant disturbances via distributed integral action," *Proceedings of the American Control Conference*, vol. 2015-July, pp. 62–67, 2015.

[45] M. Andreasson, H. Sandberg, D. V. Dimarogonas, and K. H. Johansson, "Distributed integral action: Stability analysis and frequency control of power systems," *2012 IEEE 51st IEEE Conference on Decision and Control (CDC)*, pp. 2077–2083, 2012.

[46] D. Burbano and M. Di Bernardo, "Consensus and synchronization of complex networks via proportional-integral coupling," *Proceedings - IEEE International Symposium on Circuits and Systems*, no. 1, pp. 1796–1799, 2014.

[47] D. A. Burbano Lombana and M. Di Bernardo, "Distributed PID control for consensus of homogeneous and heterogeneous networks," *IEEE Transactions on Control of Network Systems*, vol. 2, no. 2, pp. 154–163, 2015.

[48] D. Burbano and M. Bernardo, "Multiplex PI control for consensus in networks of heterogeneous linear agents," *Automatica*, vol. 67, pp. 310–320, 2016.

[49] D. Burbano and M. Bernardo, "Multilayer Proportional-Integral Consensus of Heterogeneous Multi-agent Systems," *Conference on Decision and Control (CDC)*, no. Cdc, 2015.

[50] P. Kundur, N. J. Balu, and M. G. Lauby, *Power system stability and control*, vol. 7. McGraw-hill New York, 1994.

[51] J. W. Simpson-Porco, F. D??rfler, and F. Bullo, "Synchronization and power sharing for droop-controlled inverters in islanded microgrids," *Automatica*, vol. 49, no. 9, pp. 2603–2611, 2013.

[52] V. Toro and E. Mojica-Nava, "Droop-free control for networked microgrids," in *Control Applications (CCA), 2016 IEEE Conference on*, pp. 374–379, IEEE, 2016.